References

1. Conley, M. E., A. K. Dobbs, D. M. Farmer, S. Kilic, K. Paris, S. Grigoriadou, E. Coustan-Smith, V. Howard, and D. Campana. 2009. Primary B cell immunodeficiencies: comparisons and contrasts. *Annu. Rev. Immunol.* 27: 199–227.
2. Conley, M. E. 1992. Molecular approaches to analysis of X-linked immunodeficiencies. *Annu. Rev. Immunol.* 10: 215–238.
3. Pisitkun, P., J. A. Deane, M. J. Difilippantonio, T. Tarasenko, A. B. Satterthwaite, and S. Bolland. 2006. Autoreactive B cell responses to RNA-related antigens due to TLR7 gene duplication. *Science* 312: 1669–1672.
4. Wesley, J. D., M. S. Tessmer, C. Paget, F. Trottein, and L. Brossay. 2007. A Y chromosome-linked factor impairs NK T development. *J. Immunol.* 179: 3480–3487.
5. Monroe, J. G., and K. Dorshkind. 2007. Fate decisions regulating bone marrow and peripheral B lymphocyte development. *Adv. Immunol.* 95: 1–50.
6. Kikuchi, K., A. Y. Lai, C. L. Hsu, and M. Kondo. 2005. IL-7 receptor signaling is necessary for stage transition in adult B cell development through up-regulation of EBF. *J. Exp. Med.* 201: 1197–1203.
7. Quong, M. W., W. J. Romanow, and C. Murre. 2002. E protein function in lymphocyte development. *Annu. Rev. Immunol.* 20: 301–322.
8. Busslinger, M. 2004. Transcriptional control of early B cell development. *Annu. Rev. Immunol.* 22: 55–79.
9. Nutt, S. L., and B. L. Kee. 2007. The transcriptional regulation of B cell lineage commitment. *Immunity* 26: 715–725.
10. Malin, S., S. McManus, and M. Busslinger. 2010. STAT5 in B cell development and leukemia. *Curr. Opin. Immunol.* 22: 168–176.
11. Mandel, E. M., and R. Grosschedl. 2010. Transcription control of early B cell differentiation. *Curr. Opin. Immunol.* 22: 161–167.
12. Di Santo, J. P. 2006. Natural killer cell developmental pathways: a question of balance. *Annu. Rev. Immunol.* 24: 257–286.
13. Sun, J. C., and L. L. Lanier. 2011. NK cell development, homeostasis and function: parallels with CD8$^+$ T cells. *Nat. Rev. Immunol.* 11: 645–657.
14. Hesslein, D. G., and L. L. Lanier. 2011. Transcriptional control of natural killer cell development and function. *Adv. Immunol.* 109: 45–85.
15. Boos, M. D., Y. Yokota, G. Eberl, and B. L. Kee. 2007. Mature natural killer cell and lymphoid tissue-inducing cell development requires Id2-mediated suppression of E protein activity. *J. Exp. Med.* 204: 1119–1130.
16. Chen, S., L. C. Ndhlovu, T. Takahashi, K. Takeda, Y. Ikarashi, T. Kikuchi, K. Murata, P. P. Pandolfi, C. Riccardi, M. Ono, et al. 2008. Co-inhibitory roles for glucocorticoid-induced TNF receptor in CD1d-dependent natural killer T cells. *Eur. J. Immunol.* 38: 2229–2240.
17. Hardy, R. R., and K. Hayakawa. 2001. B cell development pathways. *Annu. Rev. Immunol.* 19: 595–621.
18. Vieira, P., and A. Cumano. 2004. Differentiation of B lymphocytes from hematopoietic stem cells. *Methods Mol. Biol.* 271: 67–76.
19. Williams, N. S., J. Klem, I. J. Puzanov, P. V. Sivakumar, M. Bennett, and V. Kumar. 1999. Differentiation of NK1.1+, Ly49+ NK cells from flt3+ multipotent marrow progenitor cells. *J. Immunol.* 163: 2648–2656.
20. Tang, Y., C. Peitzsch, H. N. Charoudeh, M. Cheng, P. Chaves, S. E. Jacobsen, and E. Sitnicka. 2012. Emergence of NK-cell progenitors and functionally competent NK-cell lineage subsets in the early mouse embryo. *Blood* 120: 63–75.
21. Raff, M. C., M. Megson, J. J. Owen, and M. D. Cooper. 1976. Early production of intracellular IgM by B-lymphocyte precursors in mouse. *Nature* 259: 224–226.
22. Bain, G., E. C. Maandag, D. J. Izon, D. Amsen, A. M. Kruisbeek, B. C. Weintraub, I. Krop, M. S. Schlissel, A. J. Feeney, M. van Roon, et al. 1994. E2A proteins are required for proper B cell development and initiation of immunoglobulin gene rearrangements. *Cell* 79: 885–892.
23. Lin, H., and R. Grosschedl. 1995. Failure of B-cell differentiation in mice lacking the transcription factor EBF. *Nature* 376: 263–267.
24. Zhuang, Y., P. Soriano, and H. Weintraub. 1994. The helix-loop-helix gene E2A is required for B cell formation. *Cell* 79: 875–884.
25. Zhang, Z., C. V. Cotta, R. P. Stephan, C. G. deGuzman, and C. A. Klug. 2003. Enforced expression of EBF in hematopoietic stem cells restricts lymphopoiesis to the B cell lineage. *EMBO J.* 22: 4759–4769.
26. Kikuchi, K., and M. Kondo. 2006. Developmental switch of mouse hematopoietic stem cells from fetal to adult type occurs in bone marrow after birth. *Proc. Natl. Acad. Sci. USA* 103: 17852–17857.
27. Jensen, C. T., S. Kharazi, C. Böiers, M. Cheng, A. Lübking, E. Sitnicka, and S. E. Jacobsen. 2008. FLT3 ligand and not TSLP is the key regulator of IL-7-independent B-1 and B-2 B lymphopoiesis. *Blood* 112: 2297–2304.
28. Sitnicka, E., C. Brakebusch, I. L. Martensson, M. Svensson, W. W. Agace, M. Sigvardsson, N. Buza-Vidas, D. Bryder, C. M. Cilio, H. Ahlenius, et al. 2003. Complementary signaling through flt3 and interleukin-7 receptor alpha is indispensable for fetal and adult B cell genesis. *J. Exp. Med.* 198: 1495–1506.
29. Carvalho, T. L., T. Mota-Santos, A. Cumano, J. Demengeot, and P. Vieira. 2001. Arrested B lymphopoiesis and persistence of activated B cells in adult interleukin 7(-/-)- mice. *J. Exp. Med.* 194: 1141–1150.
30. Suzuki, H., G. S. Duncan, H. Takimoto, and T. W. Mak. 1997. Abnormal development of intestinal intraepithelial lymphocytes and peripheral natural killer cells in mice lacking the IL-2 receptor beta chain. *J. Exp. Med.* 185: 499–505.
31. Kennedy, M. K., M. Glaccum, S. N. Brown, E. A. Butz, J. L. Viney, M. Embers, N. Matsuki, K. Charrier, L. Sedger, C. R. Willis, et al. 2000. Reversible defects in natural killer and memory CD8 T cell lineages in interleukin 15-deficient mice. *J. Exp. Med.* 191: 771–780.
32. Vosshenrich, C. A., T. Ranson, S. I. Samson, E. Corcuff, F. Colucci, E. E. Rosmaraki, and J. P. Di Santo. 2005. Roles for common cytokine receptor gamma-chain-dependent cytokines in the generation, differentiation, and maturation of NK cell precursors and peripheral NK cells in vivo. *J. Immunol.* 174: 1213–1221.
33. Wang, J. H., A. Nichogiannopoulou, L. Wu, L. Sun, A. H. Sharpe, M. Bigby, and K. Georgopoulos. 1996. Selective defects in the development of the fetal and adult lymphoid system in mice with an Ikaros null mutation. *Immunity* 5: 537–549.
34. Ng, S., C. Fanta, M. Okam, and A. S. Bhatt. 2011. NK-cell and B-cell deficiency with a thymic mass. *N. Engl. J. Med.* 364: 586–588.

Hepatology Research

Hepatology Research 2013 doi: 10.1111/hepr.12168

Short Communication

Sequential analysis of amino acid substitutions with hepatitis B virus in association with nucleoside/nucleotide analog treatment detected by deep sequencing

Masashi Ninomiya,[1] Yasuteru Kondo,[1] Tetsuya Niihori,[2] Takeshi Nagashima,[3] Takayuki Kogure,[1] Eiji Kakazu,[1] Osamu Kimura,[1] Yoko Aoki,[2] Yoichi Matsubara[2] and Tooru Shimosegawa[1]

[1]*Division of Gastroenterology, Tohoku University Hospital,* [2]*Department of Medical Genetics, and* [3]*Division of Cell Proliferation, Tohoku University Graduate School of Medicine, Sendai, Japan*

Taking nucleoside/nucleotide analogs is a major antiviral therapy for chronic hepatitis B infection. The problem with this treatment is the selection for drug-resistant mutants. Currently, identification of genotypic drug resistance is conducted by molecular cloning sequenced by the Sanger method. However, this methodology is complicated and time-consuming. These limitations can be overcome by deep sequencing technology. Therefore, we performed sequential analysis of the frequency of drug resistance in one individual, who was treated with lamivudine on-and-off therapy for 2 years, by deep sequencing. The lamivudine-resistant mutations at rtL180M and rtM204V and the entecavir-resistant mutation at rtT184L were detected in the first subject. The lamivudine- and entecavir-resistant strain was still detected in the last subject. However, in the deep sequencing analysis, rt180 of the first subject showed a mixture in 76.9% of the methionine and in 23.1% of the leucine, and rt204 also showed a mixture in 69.0% of the valine and 29.8% of the isoleucine. During the treatment, the ratio of resistant mutations increased. At rt184, the resistant variants were detectable in 58.7% of the sequence, with the replacement of leucine by the wild-type threonine in the first subject. Gradually, entecavir-resistant variants increased in 82.3% of the leucine in the last subject. In conclusion, we demonstrated the amino acid substitutions of the serial nucleoside/nucleotide analog resistants. We revealed that drug-resistant mutants appear unchanged at first glance, but actually there are low-abundant mutations that may develop drug resistance against nucleoside/nucleotide analogs through the selection of dominant mutations.

Key words: amino acid substitutions, deep sequencing, hepatitis B virus, nucleoside/nucleotide analog resistants

Approximately 350–400 million patients are chronically infected with hepatitis B virus (HBV) globally, and the disease has caused epidemics in East Asia.[1,2] In Japan, approximately 1.5 million people are infected with HBV.[3] Chronic hepatitis B (CHB) increases the risk of liver cirrhosis and hepatocellular carcinoma.[4]

Hepatitis B virus is a DNA virus of 3.2 kb surrounded by an envelope of the surface protein (hepatitis B surface antigen [HBsAg]) and it has a circular genome of partially double-stranded DNA.[5] Once the HBV invades into hepatic cells, genomic DNA is transferred to the cell nucleus.[6] In the nucleus, the genomic DNA is converted to a stable intrahepatic reservoir of cccDNA. The cccDNA replicates through an RNA intermediate form by reverse transcription.[7] The purpose of CHB therapy is to achieve sustained suppression of HBV replication and the remission of liver disease. However, cccDNA is resistant to treatment and is not completely eradicated by currently available medications.[8,9] Taking nucleoside/nucleotide analogs (NA) is a major antiviral therapy for the treatment of CHB.[4] Therapies with NA available in Japan include lamivudine (LAM), adefovir dipivoxil (ADV) and entecavir (ETV). They inhibit viral polymerase activity by interfering with the priming of reverse transcription and elongation of the viral minus or plus strand DNA.[10–12] Most patients have chemical and virological responses, but these treatments are hampered by the selection of drug-resistant mutants, leading

Correspondence: Dr Yasuteru Kondo, Division of Gastroenterology, Tohoku University Hospital, 1-1 Seiryo, Aoba-ku, Sendai 980-8574, Japan. Email: yasuteru@ebony.plala.or.jp

The GenBank/EMBL/DDBJ accession numbers for the nucleotide sequences reported in this paper are AB820840-AB820852.

Received 7 March 2013; revision 14 May 2013; accepted 20 May 2013.

to a loss of efficacy, viral relapse and exacerbations of hepatitis after discontinuation.[13]

In the present study, the region of codon rt148 to rt 208 in the polymerase open reading frame was found to include the reported relevant NA-resistant amino acid substitutions. Resistance to LAM has been mapped to the YMDD locus in the C domain of rtM204I/V and is sometimes associated with compensatory mutations in the B domain of rtL180M and/or rtV173L.[14–16] The mutations common to LMV confer cross-resistance and reduced sensitivity to ETV but not to ADV. ETV resistance has been mapped to the B domain with rtI169T, rtL180M and/or rtT184S/A/I/L/F/G/C/M, C domain with rtS202C/G/I and rtM204V/I, and E domain of rtM250I/L/V. The three amino acid substitutions of rtL180 + rtM204 and either rtT184, rtS202 or rtM250 are required for ETV resistance to develop.[17–19] The mutations in the B domain of rtA181S/T/V and D domain of rtN236T were reported to be associated with ADV resistance.[20,21]

Currently, identification of HBV genotypic NA resistance is mainly conducted by polymerase chain reaction (PCR) amplification with Sanger direct sequencing. However, with this method it is difficult to measure the frequencies of each mutation, and it is impossible to detect several mutations combined in the same sequence. It is necessary to find the frequencies of NA-resistant amino acid substitutions, because the secondary compensatory mutations associated with primary NA resistance may restore replication defects or even give rise to multidrug-resistant variants.[19] As an alternative to Sanger direct sequencing, molecular cloning can analyze single viral DNA molecules. However, this methodology is complicated and time-consuming, because analysis of three-digit clones is required to detect variants present in several percent of quasispecies. These limitations can now be overcome by deep sequencing technology.[22] Genetic diversity plays a key role in the NA treatment of HBV infection. Therefore, using this technology, minor HBV variants can be detected, including those with combinations of nucleotide changes in the same period. Detecting low-frequency NA resistants will be important for choosing the NA treatment. In this study, we investigated the transition frequency of amino acid substitutions in NA resistants, in one case using deep sequencing during 2 years of ETV and ADV combination treatment.

A 42-year-old man, diagnosed with CHB infection in June 2005, was treated with LAM on-and-off therapy for 2 years. In HIV-infected patients, on-and-off antiretroviral therapy increased the risk of drug resistance compared with continuous therapy.[23] The HBV DNA levels had gradually increased and ETV treatment was begun in November 2007, but the HBV DNA levels did not decrease, and the treatment was stopped in November 2009. The level of serum transaminase was not elevated at that period. In April 2010, he was seen for the first time in our hospital. The patient was asymptomatic but showed an elevation of transaminase. The following clinical data was indicated: aspartate aminotransferase, 66 IU/L; alanine aminotransferase (ALT), 178 IU/L; positive for HBsAg, hepatitis B e-antigen (HBeAg) and hepatitis B core antibody; HBV genotype C; HBV DNA levels of 1.0×10^8 copies/mL; and negative for anti-hepatitis C virus and anti-HIV. The combination of ETV (0.5 mg/day) and ADV (10 mg/day) therapy was started at that time. After 3 months of therapy, the ALT elevation (119 IU/L) still persisted. Then, the dose of ETV was increased from 0.5 mg to 1.0 mg daily from August 2010. Three months after starting ETV at a dose of 1.0 mg, ALT was at 40 IU/L and HBV DNA had decreased to 6.3×10^3 copies/mL. At the most recent follow up, ALT has remained normal and HBV DNA is at nearly an undetectable level ($<1.3 \times 10^2$ copies/mL). Of note, the serum level of HBeAg is still positive. The changes in viral load and ALT levels are presented in Figure 1(a).

To investigate mutation involved in NA resistance, six serial serum samples of HBV-P10140 (stored in April 2010), HBV-P10193 (June 2010), HBV-P10234 (July 2010), HBV-P10264 (August 2010), HBV-P11021 (January 2011) and 12-009 (January 2012) were enrolled in this study. We extracted HBV DNA by the method described previously with slight modification.[24] Nucleic acids were obtained from 100 μL serum samples using SMITEST EX-R&D (Medical & Biological Laboratories, Nagoya, Japan) and nested PCR was conducted in the presence of PrimeSTAR HS DNA polymerase (TaKaRa Bio, Shiga, Japan) four with primers targeting the polymerase gene of HBV genomes (Table 1). The amplification product of the first-round PCR was 457 bp (nt 596–1052), and that of the second-round PCR was 390 bp (nt 610–999): the nucleotide numbers are in accordance with a genotype B HBV isolate of 3215 nt (accession no. AB010289). The first-round PCR with primers B034 and B037 was conducted for 30 cycles and the second-round PCR for 25 cycles with primers B035 and B036 (Table 1). The second-round PCR amplicons were sequenced directly on both strands using a BigDye Terminator version 3.1 Cycle Sequencing Kit (Applied Biosystems, Foster City, CA, USA) on a 3500xL Genetic Analyzer (Applied Biosystems).

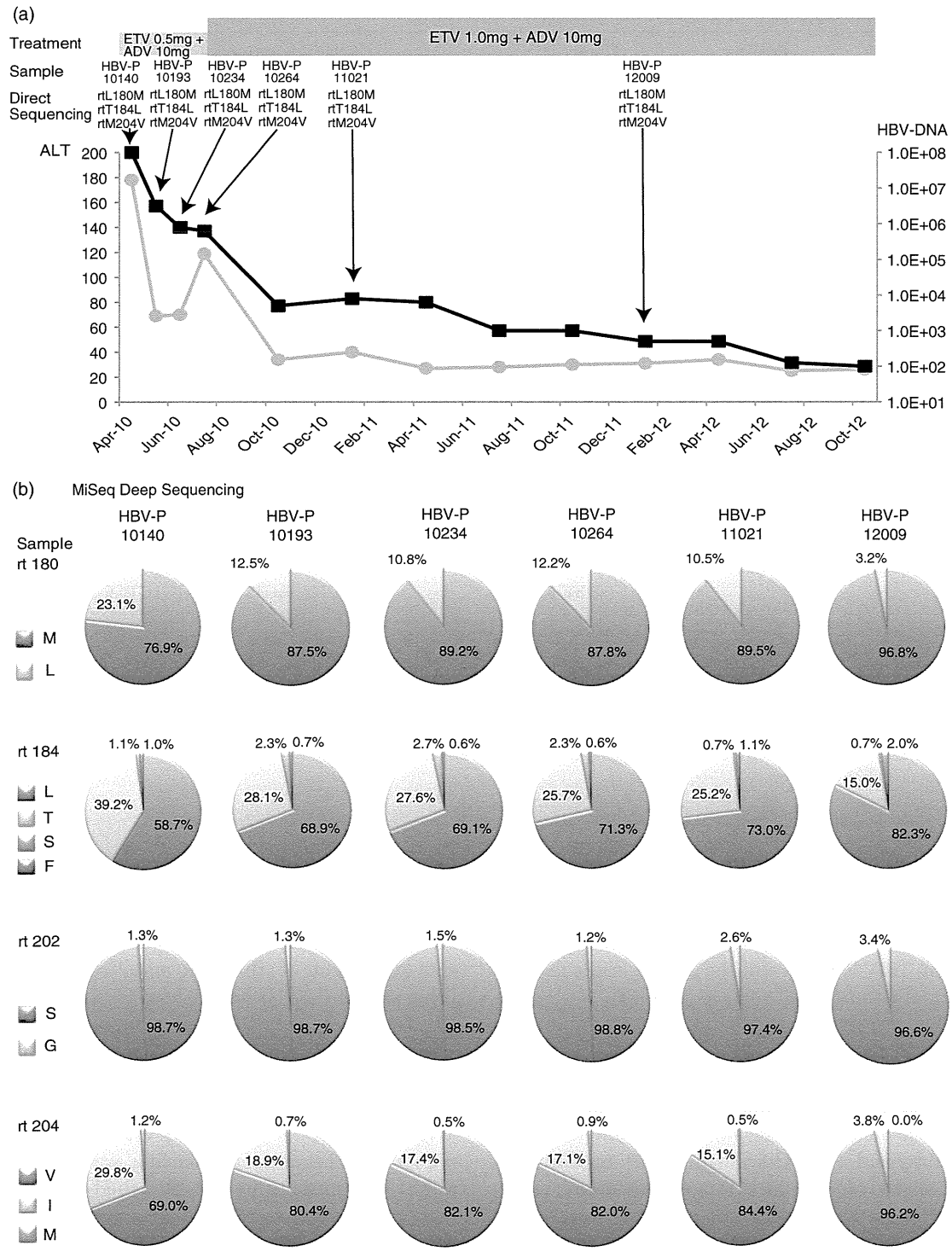

Figure 1 Clinical stage and amino acid substitutions of hepatitis B virus (HBV) resistants. (a) Evolution of HBV DNA viral load, alanine aminotransferase (ALT) levels and resistant HBV variants sequenced directly with Sanger methods in a patient treated sequentially with entecavir (ETV) and adefovir dipivoxil (ADV). (b) Frequency of amino acid substitutions of nucleoside/nucleotide analog (NA)-resistant HBV by MiSeq deep sequencing. M denotes methionine, L denotes leucine, T denotes threonine, V denotes valine, S denotes serine, F denotes phenylalanine, G denotes glycine and I denotes isoleucine. —■—, HBV-DNA; —●—, ALT.

Table 1 Nucleotide sequence of oligonucleotide primers

Primer	Polarity	Usage	Nucleotide sequence
B034	Sense	1st PCR	ACYTGTATTCCCATCCCATC
B037	Antisense	1st PCR	AARGCAGGRTADCCACATTG
B035	Sense	2nd PCR	CCCATCRTCYTGGGCTTTCG
B036	Antisense	2nd PCR	AATTCKYTGACATACTTTCCAATC
P5_B035	Sense	MiSeq sequence	AATGATACGGCGACCACCGAGATCTACACTC TTTCCCTACACGACGCTCTTCCGATCT*CCCA TCRTCYTGGGCTTTCG*
P7_Index1_B036	Antisense	MiSeq sequence of HBV-P10140	CAAGCAGAAGACGGCATACGAGAT***CGTGAT***G TGACTGGAGTTCAGACGTGTGCTCTTCCGA T*CTAATTCKYTGACATACTTTCCAATC*
P7_Index2_B036	Antisense	MiSeq sequence of HBV-P10193	CAAGCAGAAGACGGCATACGAGAT***ACATCG***G TGACTGGAGTTCAGACGTGTGCTCTTCCGAT *CTAATTCKYTGACATACTTTCCAATC*
P7_Index3_B036	Antisense	MiSeq sequence of HBV-P10234	CAAGCAGAAGACGGCATACGAGAT***GCCTAA***GT GACTGGAGTTCAGACGTGTGCTCTTCCGATCT *AATTCKYTGACATACTTTCCAATC*
P7_Index4_B036	Antisense	MiSeq sequence of HBV-P10264	CAAGCAGAAGACGGCATACGAGAT***TGGTCA***GTG ACTGGAGTTCAGACGTGTGCTCTTCCGATCT*AA TTCKYTGACATACTTTCCAATC*
P7_Index5_B036	Antisense	MiSeq sequence of HBV-P11021	CAAGCAGAAGACGGCATACGAGAT***CACTGT***GTG ACTGGAGTTCAGACGTGTGCTCTTCCGATCT*AA TTCKYTGACATACTTTCCAATC*
P7_Index6_B036	Antisense	MiSeq sequence of HBV-P12009	CAAGCAGAAGACGGCATACGAGAT***ATTGGC***GTGA CTGGAGTTCAGACGTGTGCTCTTCCGATCT*AATT CKYTGACATACTTTCCAATC*

Y denotes C or T, R denotes A or G, D denotes A, G or T and K denotes G or T. Italic bold letters indicate the index by multiplex sequencing. Italic letters indicate the nucleotide sequence of B035 or B036.
PCR, polymerase chain reaction.

The LAM-resistant mutations at rtL180M and rtM204V, and the ETV-resistant mutation at rtT184L in HBV-P10140 were detected by direct sequencing. The HBV-mutated LAM- and ETV-resistant strain was still detected in HBV-P12009 and the amino acid substitutions were the same in all subjects (Fig. 1a).

Next, we investigated the frequency of amino acid bases with these same six PCR amplicons by MiSeq (Illumina, San Diego, CA, USA) deep sequencing. MiSeq is the only deep sequencer that quickly integrates amplification, sequencing and data analysis in a single instrument. Compared with HiSeq (Illumina) or Illumina GA IIx, MiSeq can produce longer paired-end reads ($<2 \times 250$) with fewer gigabases of data. However, it has a large enough data volume to sequence PCR amplicons.

A second PCR was performed to attach the required sequencing adaptor for Illumina Miseq sequencing protocol as well as barcode to allow multiplexing of multiple sample libraries per sequencing lane. Six pairs of primers tailed with the adaptor and the specific index were used to amplify six first PCR amplicons. Eight cycles of PCR were performed using PrimeSTAR HS DNA polymerase. All adaptor–barcode–primers are shown in Table 1. The PCR amplicons were purified using AMPure XP beads (Beckman Coulter, Danvers, MA, USA) and the quality and quantity were checked by size range analysis using a D1K ScreenTape on the 2200 Tapestation (Agilent Technologies, Santa Clara, CA, USA). Each library was pooled in equal amounts, and a PhiX control kit (Illumina) was added to 95% of the pooled libraries. Sequencing was performed on MiSeq (Illumina) using 251-bp paired-end reads. Fastq files including demultiplexed sequence reads were generated by Miseq reporter. 251-bp paired-end reads were stripped of low quality 3′-regions using trim galore (www.bioinformatics.babraham.ac.uk/projects/trim_galore/). Sequence reads were aligned with the HBV reference sequence of Yamagata-1 (accession no. AB010289) using of Bowtie 2 (2.1.0).[25] The analysis

Table 2 Number of reads and read depth of each sample

Sample	HBV-P10140	HBV-P10193	HBV-P10234	HBV-P10264	HBV-P11021	HBV-P12009
No. of reads mapping on HBV reference	187 336	186 386	166 257	158 781	169 709	137 139
Read depth	88 985	87 825	76 775	75 296	80 190	65 095

of the read depth and base count is displayed using GATK (www.broadinstitute.org/gatk/).

A total of 1 005 608 validated reads corresponding to six serial samples were analyzed by deep sequencing. The mean number of reads mapping on the HBV reference was 167 601 and the mean depth of each case was 79 028 (Table 2). The nine most variable amino acid substitutions, rt169, rt173, rt180, rt181, rt184, rt202, rt204, rt236 and rt250, known to be associated with NA resistance, were examined. The problem was how to differentiate true mutations from sequencing error in the obtained reads. Nishijima *et al.* tried to determine the PCR amplicon of the HBV genome derived from the expression plasmid to take the PCR-induced errors as well as sequencing errors into consideration. They described that the mean error rate was 0.034%, with the distribution of the per-nucleotide error rate ranging 0–0.13%.[26] Therefore, mutations over 1.0% were considered to be valid. First, rt180 of HBV-P10140 showed mixed variants in 76.9% of methionine with LAM-resistant mutations and in 23.1% of wild type with leucine, and rt204 also showed mixed variants in 69.0% of valine and 29.8% of isoleucine with LAM-resistant mutations, and in only 1.2% of wild-type methionine. During the NA treatment, the ratio of resistance mutations was increased, and rt180 of HBV-P12009 showed mixed variants in 96.8% of methionine with LAM-resistant mutations and rt204 also showed mixed variants in 96.2% of valine with LAM-resistant mutations. At rt184, related to ETV resistance, the resistant variants were detectable in 58.7% of the sequence, with replacement of leucine by wild-type threonine in HBV-P10140. Gradually, ETV-resistant variants increased and were detected in 82.3% of leucine in HBV-P12009. In addition, at rt202, the ration of serine with ETV mutants was increased from 1.3% to 3.4% during the treatment with NA (Fig. 1b). Of note, at rt169, rt173, rt181, rt236 and rt250, there were no NA-resistant mutations.

Then, we investigated the existence of drug-resistant HBV clones that could latently develop in patients. We enrolled seven patients treated with continuous NA for up to 2 years but in whom there was continual detection of viral copies in serum in this trial. Direct Sanger sequencing detected LAM-resistant mutations in five of the seven subjects. They had the following mutations: (i) rtL180M + rtM204V and (ii) rt180M and no mutations were found at rtV173L. However, by deep sequencing, in four subjects there was part of a mixture with rtL180L/M (35.4%/64.6%) and rtM204M/V (35.2%/64.8%) in HBV-P10036, with rtL180L/M (10.6%/86.8%) and rtM204M/V/I (0.0%/75.5%/24.5%) in HBV-P12043, with rtL180L/M (19.5%/80.5%) and rtM204M/V/I (4.4%/79.5%/16.1%) in HBV-P13064 and with rtL180L/M (23.4%/76.6%), rtM204M/V/I (23.2%/41.6%/35.2%) and one secondary minority variant of rtV173V/L (55.4%/44.6%) in HBV-P13061. Next, an ADV-resistant mutation of rtA181V was detected in two subjects by Sanger sequencing, and was present in 100.0% in HBV-P07061 and in 35.3% in HBV-P08463 by deep sequencing. In addition, minority variant ADV-resistant mutations were detected with 8.5% of rtA181V and with 14.5% of rtN236T in HBV-P10036, and with 2.1% of rtA181V in HBV-P13064. Of note, an ETV-resistant mutation appeared only in one subject with rtT184L by Sanger sequencing, while some low frequency ETV-resistant mutations were detected in four subjects by deep sequencing (Table 3). Therefore, the continual viremia of HBV treated with NA for long term may lead to NA-resistant mutations.

In conclusion, we demonstrated the amino acid substitutions of serial NA-resistant HBV by Sanger sequencing and MiSeq deep sequencing. We revealed that NA-resistant mutants appear unchanged at a glance but suggest the existence of low-abundant mutant clones that may develop drug resistance against NA through the selection of dominant mutations. The viral loads have decreased, but the effect of ETV is expected to be reduced. Further analysis by deep sequencing technologies is necessary to understand the significance and clinical relevance of viral mutations in the pathophysiology of NA-resistant HBV infection.

Table 3 HBV NA-resistant mutations detected by Sanger sequencing and deep sequencing

Sample	Treatment	HBV DNA (log copies/mL)	NA-resistant mutations	
			Sanger sequence	Deep sequence
HBV-P07061	LAM + ADV	5.0	A181V	**A181V (100.0%)**
HBV-P10036	ETV	2.5	L180M, M204V	V173M (1.3%), **L180M (64.6%)**, **A181V (8.5%)**, **T184S (4.5%)**, **S202C (2.3%)**, **M204V (64.8%)**, **N236T (14.3%)**
HBV-P08463	ETV	3.4	A181V	**A181V (35.3%)**
HBV-P12043	ETV	4.7	L180M, M204V	V173M (4.4%), **V173L (2.7%)**, **L180M (86.8%)**, L180Q (2.6%), **T184L (27.9%)**, **T184M (5.1%)**, **S202G (16.6%)**, **M204V (75.5%)**, **M204I (24.5%)**
HBV-P12081	LAM + ADV	2.9	L180M, T184L, M204V	I169A (25.4%), **L180M (100.0%)**, **T184L (100.0%)**, **M204V (100.0%)**
HBV-P13064	ETV	7.1	L180M, M204V	V173M (12.9%), **L180M (80.5%)**, **A181V (2.1%)**, **A181T (3.6%)**, **M204V (79.5%)**, **M204I (16.1%)**, **M250L (2.8%)**
HBV-P13061	ETV	2.3	L180M	**V173L (44.6%)**, **L180M (76.6%)**, **M204V (41.6%)**, **M204I (35.2%)**, **M250L (1.3%)**

Mutations in bold type at deep sequence section showed NA-resistant mutations that have already been reported.
ADV, adefovir dipivoxil; ETV, entecavir; HBV, hepatitis B virus; LAM, lamivudine; NA, nucleoside/nucleotide analog.

REFERENCES

1 EASL clinical practice guidelines: management of chronic hepatitis B virus infection. *J Hepatol* 2012; **57**: 167–85.
2 Pan CQ, Hu KQ, Tsai N. Long-term therapy with nucleoside/nucleotide analogues for chronic hepatitis B in Asian patients. *Antivir Ther* 2012; doi: 10.3851/IMP2481. [Epub ahead of print].
3 Yokosuka O, Kurosaki M, Imazeki F *et al.* Management of hepatitis B: consensus of the Japan Society of Hepatology 2009. *Hepatol Res* 2011; **41**: 1–21.
4 Lok ASF, McMahon BJ. Chronic hepatitis B: update 2009. *Hepatology* 2009; **50**: 661–2.
5 Zuckerman AJ. Hepatitis viruses. In: Baron S, ed. *Medical Microbiology*, 4th edn. Galveston (TX): University of Texas Medical Branch at Galveston, 1996; Chapter 70.
6 Kann M, Bischof A, Gerlich WH. In vitro model for the nuclear transport of the hepadnavirus genome. *J Virol* 1997; **71**: 1310–16.
7 Locarnini S. Molecular virology of hepatitis B virus. *Semin Liver Dis* 2004; **24** (Suppl 1): 3–10.
8 Werle-Lapostolle B, Bowden S, Locarnini S *et al.* Persistence of cccDNA during the natural history of chronic hepatitis B and decline during adefovir dipivoxil therapy. *Gastroenterology* 2004; **126**: 1750–8.
9 Wong DK, Yuen MF, Ngai VW, Fung J, Lai CL. One-year entecavir or lamivudine therapy results in reduction of hepatitis B virus intrahepatic covalently closed circular DNA levels. *Antivir Ther* 2006; **11**: 909–16.
10 Severini A, Liu XY, Wilson JS, Tyrrell DL. Mechanism of inhibition of duck hepatitis B virus polymerase by (-)-beta-L-2′,3′-dideoxy-3′-thiacytidine. *Antimicrob Agents Chemother* 1995; **39**: 1430–5.
11 Seigneres B, Aguesse-Germon S, Pichoud C *et al.* Duck hepatitis B virus polymerase gene mutants associated with resistance to lamivudine have a decreased replication capacity in vitro and in vivo. *J Hepatol* 2001; **34**: 114–22.
12 Seifer M, Hamatake RK, Colonno RJ, Standring DN. In vitro inhibition of hepadnavirus polymerases by the triphosphates of BMS-200475 and lobucavir. *Antimicrob Agents Chemother* 1998; **42**: 3200–8.
13 Inada M, Yokosuka O. Current antiviral therapies for chronic hepatitis B. *Hepatol Res* 2008; **38**: 535–42.
14 Allen MI, Deslauriers M, Andrews CW *et al.* Identification and characterization of mutations in hepatitis B virus resistant to lamivudine. Lamivudine Clinical Investigation Group. *Hepatology* 1998; **27**: 1670–7.
15 Fu L, Cheng YC. Role of additional mutations outside the YMDD motif of hepatitis B virus polymerase in L(-)SddC (3TC) resistance. *Biochem Pharmacol* 1998; **55**: 1567–72.
16 Fu L, Liu SH, Cheng YC. Sensitivity of L-(-)2,3-dideoxythiacytidine resistant hepatitis B virus to other antiviral nucleoside analogues. *Biochem Pharmacol* 1999; **57**: 1351–9.
17 Tenney DJ, Levine SM, Rose RE *et al.* Clinical emergence of entecavir-resistant hepatitis B virus requires additional substitutions in virus already resistant to Lamivudine. *Antimicrob Agents Chemother* 2004; **48**: 3498–507.
18 Tenney DJ, Rose RE, Baldick CJ *et al.* Long-term monitoring shows hepatitis B virus resistance to entecavir in

nucleoside-naive patients is rare through 5 years of therapy. *Hepatology* 2009; **49**: 1503–14.
19 Locarnini S. Primary resistance, multidrug resistance, and cross-resistance pathways in HBV as a consequence of treatment failure. *Hepatol Int* 2008; **2**: 147–51.
20 Bartholomeusz A, Tehan BG, Chalmers DK. Comparisons of the HBV and HIV polymerase, and antiviral resistance mutations. *Antivir Ther* 2004; **9**: 149–60.
21 Yatsuji H, Suzuki F, Sezaki H *et al.* Low risk of adefovir resistance in lamivudine-resistant chronic hepatitis B patients treated with adefovir plus lamivudine combination therapy: two-year follow-up. *J Hepatol* 2008; **48**: 923–31.
22 Ninomiya M, Ueno Y, Funayama R *et al.* Use of illumina deep sequencing technology to differentiate hepatitis C virus variants. *J Clin Microbiol* 2012; **50**: 857–66.
23 Danel C, Moh R, Chaix ML *et al.* Two-months-off, four-months-on antiretroviral regimen increases the risk of resistance, compared with continuous therapy: a randomized trial involving West African adults. *J Infect Dis* 2009; **199**: 66–76.
24 Takahashi M, Nishizawa T, Gotanda Y *et al.* High prevalence of antibodies to hepatitis A and E viruses and viremia of hepatitis B, C, and D viruses among apparently healthy populations in Mongolia. *Clin Diagn Lab Immunol* 2004; **11**: 392–8.
25 Langmead B, Salzberg SL. Fast gapped-read alignment with Bowtie 2. *Nat Methods* 2012; **9**: 357–9.
26 Nishijima N, Marusawa H, Ueda Y *et al.* Dynamics of hepatitis B virus quasispecies in association with nucleos(t)ide analogue treatment determined by ultra-deep sequencing. *PLoS ONE* 2012; **7**: e35052.

nature chemical biology

ARTICLE

PUBLISHED ONLINE: 15 DECEMBER 2013 | DOI: 10.1038/NCHEMBIO.1410

VMAT2 identified as a regulator of late-stage β-cell differentiation

Daisuke Sakano[1], Nobuaki Shiraki[1], Kazuhide Kikawa[1,2], Taiji Yamazoe[1], Masateru Kataoka[1], Kahoko Umeda[1], Kimi Araki[3], Di Mao[4], Shirou Matsumoto[2], Naomi Nakagata[5], Olov Andersson[6,7], Didier Stainier[6,8], Fumio Endo[2], Kazuhiko Kume[1,10], Motonari Uesugi[4] & Shoen Kume[1,9]*

Cell replacement therapy for diabetes mellitus requires cost-effective generation of high-quality, insulin-producing, pancreatic β cells from pluripotent stem cells. Development of this technique has been hampered by a lack of knowledge of the molecular mechanisms underlying β-cell differentiation. The present study identified reserpine and tetrabenazine (TBZ), both vesicular monoamine transporter 2 (VMAT2) inhibitors, as promoters of late-stage differentiation of *Pdx1*-positive pancreatic progenitor cells into *Neurog3* (referred to henceforth as *Ngn3*)-positive endocrine precursors. VMAT2-controlled monoamines, such as dopamine, histamine and serotonin, negatively regulated β-cell differentiation. Reserpine or TBZ acted additively with dibutyryl adenosine 3′,5′-cyclic AMP, a cell-permeable cAMP analog, to potentiate differentiation of embryonic stem (ES) cells into β cells that exhibited glucose-stimulated insulin secretion. When ES cell-derived β cells were transplanted into AKITA diabetic mice, the cells reversed hyperglycemia. Our protocol provides a basis for the understanding of β-cell differentiation and its application to a cost-effective production of functional β cells for cell therapy.

Pancreatic cells arise from definitive endoderm and Pdx1-positive (Pdx1+) pancreatic progenitor cells[1], which proliferate and give rise to all three pancreatic lineages: acini, ducts and endocrine islets[2]. Endocrine precursors are characterized by the transient expression of the basic helix-loop-helix transcription factor neurogenin 3 (Ngn3, also known as Neurog3)[2]. Previous studies showed that Ngn3 specifically establishes the endocrine lineages and that loss of Ngn3 precludes endocrine cell development[2,3]. Production of islet cells occurs through the concerted activation of a combination of transcription factors[4]. However, the coordination of cell fate decisions remains poorly understood.

The prevalence of diabetes mellitus in many populations is high, and development of cell replacement therapy through generation of β cells from ES cells is a research priority. Recent studies have shown that mouse or human ES cells can be induced to recapitulate embryonic development of the pancreas[5]. Studies on ES cell differentiation into endodermal or pancreatic cell lineages have shown that stimulation with activin, FGF or retinoic acid, in addition to inhibition of hedgehog signaling by KAAD-cyclopamine, promotes the differentiation into endoderm or pancreatic fates[6,7]. New signal pathways that promote ES cell differentiation into endodermal[8] or pancreatic[9] lineages have been discovered through large-scale screening of cell-permeable, bioactive small molecules. However, it is still difficult to derive mature β cells that secrete insulin in a glucose-dependent manner. A better understanding is needed of the underlying molecular mechanisms that control the late stages of β-cell development, in which Pdx1+ pancreatic progenitor cells develop into Ngn3+ endocrine progenitor cells and insulin-positive (Ins+) β cells and then further differentiate into mature β cells capable of glucose-stimulated insulin secretion (GSIS).

Here, we identified reserpine and TBZ as potent promoters of pancreatic progenitor cell differentiation into functional β cells. This study highlights the use of chemical compound libraries for the identification of new developmental pathways that control progenitor cell differentiation into mature β cells.

RESULTS

Reserpine and TBZ increase Ins+ cells

The present study used large-scale screening of chemical compounds with an ES cell line, SK7, that expresses GFP under the *Pdx1* promoter[10,11]. The *Pdx1*-GFP ES cell line is useful because the expression of *Pdx1* is biphasic (**Fig. 1a**), which enabled the detection of early-stage Pdx1+ pancreatic progenitors and late-stage Pdx1+ Ins+ β cells . We optimized the culture to promote modest basal differentiation with high reproducibility, so that the markers *Sox17*, *Pdx1*, *Ngn3* and *Ins1* were sequentially expressed (**Fig. 1a**).

To screen for compounds that potentiate the differentiation of ES cell–derived Pdx1+ pancreatic progenitor cells into insulin-expressing cells, we tested a library of 1,120 biologically active compounds arrayed as single compounds in DMSO on cultures, starting on day 11 after confirming the appearance of *Pdx1*-GFP+ cells and conducting the assay on day 17 (**Fig. 1a**). Candidate compounds that increased both *Ins1* expression and the number of Ins+ cells relative to vehicle (1% DMSO) were selected as primary hits. The coefficient of variation of this screen was 0.36 ± 0.0447 (± s.d.), which was difficult to minimize further owing to the long assay

[1]Department of Stem Cell Biology, Institute of Molecular Embryology and Genetics, Kumamoto University, Kumamoto, Japan. [2]Department of Pediatrics, Graduate School of Medical Sciences, Kumamoto University, Kumamoto, Japan. [3]Laboratory of Developmental Genetics, Institute of Resource Development and Analysis, Kumamoto University, Kumamoto, Japan. [4]Institute for Chemical Research and Institute for Integrated Cell-Material Sciences, (WPI-iCeMS), Kyoto University, Kyoto, Japan. [5]Division of Reproductive Engineering, Center for Animal Resources and Development, Kumamoto University, Kumamoto, Japan. [6]Department of Cell and Molecular Biology, Karolinska Institute, Stockholm, Sweden. [7]Department of Biochemistry and Biophysics, University of California–San Francisco, San Francisco, California, USA. [8]Department of Developmental Genetics, Max Planck Institute for Heart and Lung Research, Bad Nauheim, Germany. [9]Program for Leading Graduate Schools, Health Life Science Interdisciplinary and Global Oriented (HIGO) Program, Kumamoto University, Kumamoto, Japan. [10]Present address: Department of Neuropharmacology, Graduate School of Pharmaceutical Sciences, Nagoya City University, Nagoya, Japan. *e-mail: skume@kumamoto-u.ac.jp

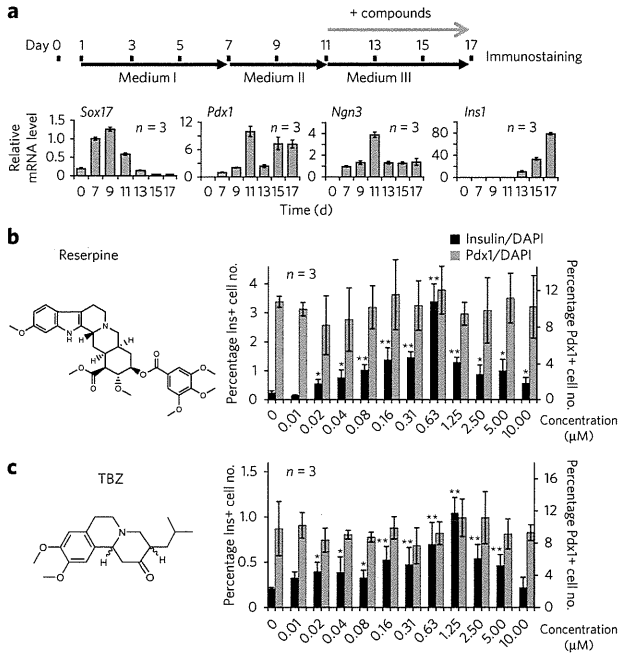

Figure 1 | Reserpine identified as a chemical that enhanced ES cell differentiation into pancreatic β cells. Using a high-throughput screening system, a chemical library was screened, and reserpine was identified as a hit chemical. (**a**) A high-throughput screening system for chemicals that enhance differentiation into β cells. Transcript expressions of *Sox17*, *Pdx1*, *Ngn3* and *Ins1* are expressed as fold change relative to control on day 7. (**b**,**c**) Reserpine (**b**) and TBZ (**c**) (chemical structure shown at left) increased the number of β cells relative to the total number of DAPI-stained cells (black bars) without affecting Pdx1+ cells (light gray bars). In **a**–**c**, data shown are mean ± s.d. ($n = 3$); significant differences between treatment and control at $^*P < 0.05$ and $^{**}P < 0.01$ are shown (two-tailed paired Student's *t*-test).

period. To overcome this, we investigated dose dependencies of the hit chemicals as a secondary screen. Of our hit compounds, the indole alkaloid antipsychotic and antihypertensive drug reserpine demonstrated the strongest effect. Reserpine increased the proportion of Ins+ cells in a concentration-dependent manner without altering the *Pdx1*-GFP+ cell ratio (**Fig. 1b**). Reserpine is known to deplete monoamines from secretory vesicles by blocking uptake into monoamine secretary granules, mediated by VMAT proteins[12–15]. Because human pancreatic β cells express the isoform VMAT2 (refs. 16–19), we also tested another VMAT2 inhibitor, TBZ, which also increased the amount of insulin-expressing cells in a dose-dependent manner (**Fig. 1c**). The half-maximal effective concentration (EC_{50}) values of reserpine and TBZ were 0.19 μM and 0.22 μM, respectively. The concentrations that led to 50% cell death (TD_{50}) were 1.56 μM reserpine and 5.98 μM TBZ. In a separate experiment, we treated cells with 0.63 μM reserpine or 1.25 μM TBZ (**Supplementary Results**, **Supplementary Fig. 1**). We confirmed the increases in the percentage of Ins+ cells out of the total cell numbers versus the untreated cells and in the relative *Ins1* mRNA levels (by real-time PCR) (**Supplementary Fig. 1**). These results suggested that VMAT2 is the candidate target molecule of reserpine and TBZ, which has a pivotal role in the differentiation of ES cells into Ins-expressing cells.

VMAT2 inhibited differentiation into Ins+ cells

To identify the role of VMAT2 in differentiation of ES cells into pancreatic β cells, we performed a knockdown of VMAT2. We established two VMAT2-knockdown SK7 cell lines, VMAT2KD1 and VMAT2KD2, using lentiviral short hairpin RNA (shRNA) (**Fig. 2a**). VMAT2KD2 exhibited lower *Slc18a2* (henceforth referred to as *Vmat2*) expression than VMAT2KD1 (**Fig. 2a**) and showed greater increases in the number of β cells and level of *Ins1* transcription (**Fig. 2b**). These results indicated that reserpine- or TBZ-mediated VMAT2 inhibition led to an enhancement of differentiation into Ins+ cells. Therefore, VMAT2-mediated monoamine storage functions as a negative regulator of differentiation into Ins+ cells. Pancreatic islets have an isozyme of the monoamine-catabolizing enzyme, monoamine oxidase B (MAO_B)[20]. We then tested the effects of application of pargyline, an MAO_B inhibitor (MAO_{Bi}), to stabilize the monoamines and increase intracellular monoamines. Indeed, application of pargyline had an inhibitory effect on the number of β cells and the level of *Ins1* expression, and reserpine counteracted the inhibitory effect of MAO_{Bi} (**Supplementary Fig. 2**). Moreover, the number and expression level of *Pdx1*-GFP+ cells was unaffected (**Supplementary Fig. 2**), similarly to treatment with reserpine and TBZ (**Fig. 1b**,**c**).

Monoamines such as dopamine, histamine and serotonin are known to be the substrates for VMAT2. We tested the effect of these monoamines by exogenous application and found that incubation with dopamine, histamine or serotonin from days 11–17 suppressed β-cell differentiation, with EC_{50} values of 1.25 μM (dopamine), 0.5 μM (histamine) and 0.92 μM (serotonin) (**Fig. 2c–e**). We determined the monoamine contents in the ES cell–derived cells on day 17 (**Fig. 2f–h** and **Supplementary Fig. 3a**,**b**). The dopamine content (approximately 1.3 pg/μg DNA) was approximately 100-fold higher compared to the other monoamines, whereas histamine was undetectable. Inhibition of VMAT2 with TBZ or reserpine and knockdown of *Vmat2* with shRNA significantly decreased ($P < 0.005$) monoamine contents, whereas treatment with pargyline increased it ($P < 0.01$) (**Fig. 2f**,**h** and **Supplementary Fig. 3**). The enzyme that synthesizes dopamine, tyrosine hydroxylase (Th), was expressed in the ES cells during differentiation at a level comparable to that in the embryonic pancreatic bud. By contrast, the histamine-synthesizing enzyme histidine decarboxylase (Hdc) and the serotonin-synthesizing enzyme tryptophan hydroxylase 1 (Tph1) were expressed at approximately 0.066-fold lower levels compared to those in the embryonic pancreas (**Supplementary Fig. 4a–c**). The monoamine receptors dopamine D2 (Drd2), histamine H1 (Hrh1), histamine H2 (Hrh2) and serotonin 1A (Htr1a) were expressed in day 11 and day 13 differentiated cells (**Supplementary Fig. 4d–f**). Upon addition of chemical compounds that inhibit the synthesizing enzymes for dopamine (α-methyl-tyrosine (α-MT) and L-3,4-dihydroxyphenylalanine (L-DOPA)), histamine (α-fluoromethylhistidine (α-FMH)) or serotonin (5-hydroxy tryptophan (5HTP) and carbidopa), we observed increases in Ins+ cell numbers (**Supplementary Fig. 4g–i**).

Taken together, VMAT2-controlled monoamine release exerted inhibitory effects on the differentiation of pancreatic progenitor cells into Ins+ cells. Reserpine and TBZ inhibit the uptake of monoamines into vesicular stores, which led to depletion of monoamines and potentiation of Ins+ cell differentiation.

TBZ increased differentiation into Ngn3+ cells

We then examined the effects of TBZ on marker expression in ES cell–derived cells by real-time PCR. We used TBZ instead of reserpine owing to its lower cytotoxicity; the results are expressed as fold changes compared to control treatments without chemicals at day 13. Treatment with TBZ resulted in a marked increase of *Ngn3*, *Nkx6-1* and *Ins1* transcripts on day 15 and day 17 (**Fig. 3a**). The real-time PCR results suggested that TBZ increases differentiation of ES cell–derived cells into *Ngn3*+ endocrine progenitors. To follow the transient increase of *Ngn3*+ endocrine precursors in living cells, we developed an NGP9 ES cell line from a transgenic mouse line bearing the *Ngn3*-promoter-driven eGFP transgene[21].

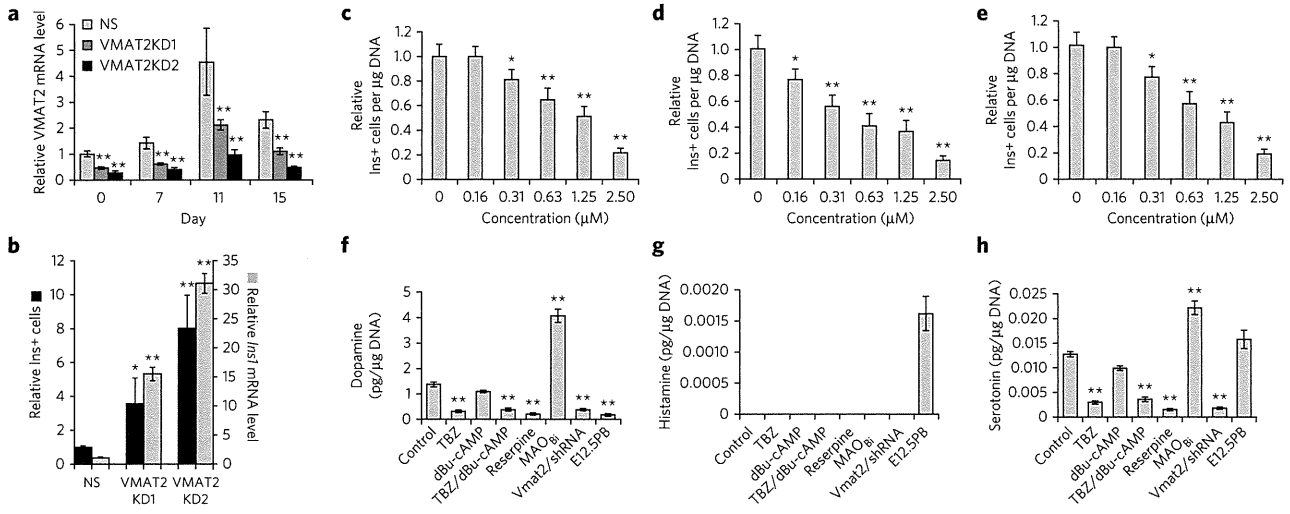

Figure 2 | VMAT2- and monoamine-dependent suppression of pancreatic β-cell differentiation. The effects of VMAT2- and monoamine-mediated inhibition on ES cell differentiation into Ins+ cells were tested, and monoamine cellular contents were determined. (**a**) Time-dependent expression of VMAT2 in VMAT2KD1 (dark gray), VMAT2KD2 (black) and control nonsilencing (NS; light gray) ES cell lines. (**b**) VMAT2KD1 and VMAT2KD2 ES cell lines yielded more Ins+ cells and *Ins1* transcripts than control NS ES cells. (**c**–**e**) Addition of monoamines, dopamine (**c**), histamine (**d**) or serotonin (**e**) suppressed differentiation of ES cells into Ins+ cells in a dose-dependent manner. (**f**–**h**) Cellular contents of dopamine (**f**), histamine (**g**) or serotonin (**h**) when added with VMAT2 inhibitors or MAO_{Bi}, treatment with both TBZ and dBu-cAMP. Control, no chemical treatment; MAO_{Bi}: 1 μM pargyline; Res: 0.63 μM reserpine; MAO_{Bi} + Res: 1 μM pargyline + 0.63 μM reserpine. For **a**–**h**, data shown are mean ± s.d. ($n = 3$); significant differences between treatment and no chemical treatment at $^*P < 0.05$ and $^{**}P < 0.01$ are shown (two-tailed paired Student's *t*-test). In **a** and **b**, black bars indicate Ins+ or *Pdx1*-GFP+ relative cell numbers, and gray bars indicate *Ins1* or *Pdx1* transcript expression relative to that in cells with no chemical treatment.

We treated the NGP9 cells with TBZ from day 11 to 13 and then performed the assay on day 13 (**Fig. 3b**). TBZ increased *Ngn3*-GFP+ cell numbers (**Fig. 3b**). These results indicate that VMAT2 signaling negatively controls differentiation into *Ngn3*-GFP+ endocrine precursors. We observed 5-ethynyl-2′-deoxyuridine (EdU) incorporation in Ngn3– cells but not in Ngn3+ cells, and TBZ addition did not increase EdU+ Ngn3+ cells, indicating that the increase in Ngn3+ cells was due to increased differentiation into Ngn3+ cells but not proliferation of Ngn3+ cells (**Fig. 3b** and **Supplementary Fig. 5a**). The Ngn3+ cells expressed Nkx2.2 and Nkx6.1 in their nuclei (**Supplementary Fig. 5b**).

We then examined whether this mechanism existed during normal embryonic development using an *in vitro* pancreas bud culture system. Upon addition of TBZ, we observed increased differentiation into insulin-, glucagon-, somatostatin- or pancreas polypeptide–expressing endocrine cells in the *Pdx1*-GFP+

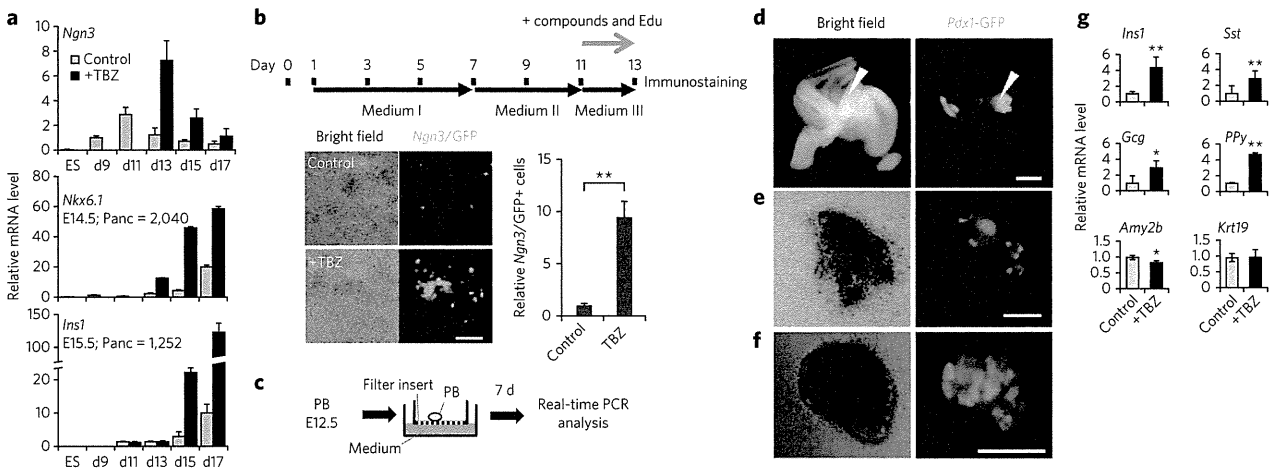

Figure 3 | VMAT2 inhibition increased differentiation into *Ngn3*-GFP+ cells. TBZ increased differentiation into *Ngn3*-GFP+ cells without increasing proliferation. (**a**) *Ngn3*, *Nkx6.1* and *Ins1* expression assayed on differentiation days (d) 13, 15 and 17, with or without (w/o) TBZ, expressed as fold change relative to control on day 13. Gray bars, no chemical (vehicle) samples; black bars, TBZ-treated samples. For all graphs, ($n = 3$). (**b**) A schematic drawing of the experimental design is shown. ES cell cultures were added with TBZ from day 11 to day 13 and assayed on day 13. Transmission or fluorescence images (left) and quantitative representations (right) of *Ngn3*-GFP+ cells without TBZ on day 13 are shown. (**c**) Schematic drawing of the experimental design. Pancreatic rudiments (PB, pancreatic bud) dissected from *Pdx1*-GFP mice at E12.5 were used for *ex vivo* culture for 7 d on filter inserts. (**d**–**f**) Transmission (left) and fluorescence (right) micrographs of explants before (**d**) and after culturing without TBZ (**e**; control DMSO) or with TBZ (**f**). (**g**) Semiquantitative real-time PCR was used to assay the expression of *Gcg*, *Sst*, *PPy*, *Amy2b* or *Krt19* after 7-d culture. Data shown are mean ± s.d. ($n = 3$), expressed as relative cell number compared to control. Scale bars, 200 μm. $^*P < 0.05$ and $^{**}P < 0.01$ (two-tailed paired Student's *t*-test).

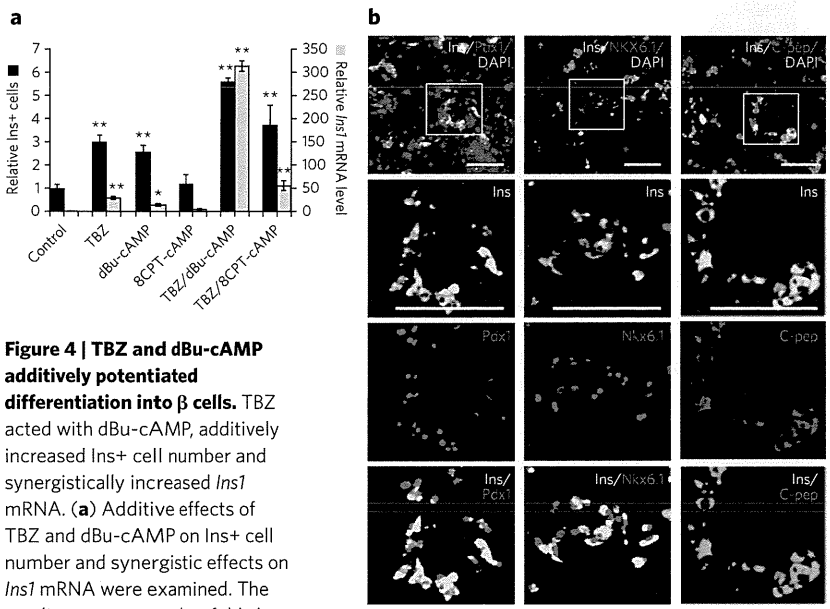

Figure 4 | TBZ and dBu-cAMP additively potentiated differentiation into β cells. TBZ acted with dBu-cAMP, additively increased Ins+ cell number and synergistically increased *Ins1* mRNA. (**a**) Additive effects of TBZ and dBu-cAMP on Ins+ cell number and synergistic effects on *Ins1* mRNA were examined. The results are expressed as fold change relative to control vehicle treatment (DMSO). By contrast, treatment with 8CPT-cAMP, a cAMP analog that specifically activates Epac2, showed no effects. Data shown are mean ± s.d. ($n = 3$), expressed as relative cell number compared to control (no chemical treatment). On the *y* axis, 1 = 0.3% Ins+ cells. (**b**) Total ES cell cultures were assayed by immunohistochemistry. Ins staining (yellow) completely overlapped with staining (red) of Pdx1, Nkx6.1 and C-peptide for *in vitro* differentiated ES cells treated on days 11–17 with TBZ and dBu-cAMP. Blue shows DAPI staining. Scale bars, 100 μm. Lower panels are enlarged pictures of the boxes in the top panels. $^*P < 0.05$ and $^{**}P < 0.01$ (two-tailed paired Student's *t*-test).

pancreatic bud explant culture (**Fig. 3c–g**). We observed a slight decrease in *Amy2b*-expressing exocrine cells but no effects on *Krt19*-expressing duct cells. These results therefore suggested that VMAT2-mediated inhibition of the progress from Pdx1+ pancreatic progenitors to Ngn3+ endocrine progenitors exists in both normal pancreatic endocrine development (**Fig. 3c–g**) and ES cell differentiation (**Fig. 3b**).

The combinatory effects of TBZ and dBu-cAMP addition

Dopamine, histamine and serotonin are considered to function through binding to their receptors. All dopamine, histamine and serotonin receptors are G protein–coupled receptors[22]. In our screen, dibutyryl adenosine 3′,5′-cAMP (dBu-CAMP), a cell-permeable cAMP analog, was identified as a compound to promote β-cell differentiation. We examined the effects of dBu-cAMP and its synergy with TBZ. TBZ or dBu-cAMP alone increased the number of Ins+ cells or the amount of *Ins1* transcript, respectively. Simultaneous addition of TBZ and dBu-cAMP caused an approximately 300-fold increase in *Ins1* transcript, which is approximately 30-fold or 15-fold the effect of single addition of TBZ or dBu-cAMP, respectively (**Fig. 4a**).

In the adult islets, cAMP is known to regulate the potentiation of insulin secretion by a protein kinase A (PKA)-dependent mechanism and a PKA-independent mechanism that involves the cAMP-binding protein Epac2 (ref. 23). As dBu-cAMP activates both pathways[24,25], we then tested a cell-permeable analog, 8CPT-cAMP, that specifically activates Epac2 but not PKA[26]. Ins+ cell number or *Ins1* gene expression did not increase with application of 8CPT-cAMP, and neither showed an additive effect after treatment with 8CPT-cAMP and TBZ. The results suggested that the potentiation of β-cell differentiation by the dBu-cAMP signaling pathway is not mediated through activation of Epac2 but possibly through PKA (**Fig. 4a**).

We then analyzed the differentiated ES cell–derived β cells generated by TBZ and dBu-cAMP treatment by immunocytochemistry. The Ins+ cells expressed Pdx1 and Nkx6.1, which are mature β cell markers. Almost all of the Pdx1+ cells were Ins+. Almost all Ins+ staining overlapped with C-peptide+ staining (**Fig. 4b**). Ins+ cells expressed Nkx2.2, Nkx6.1 and MafA (**Supplementary Fig. 6a**). We also observed *Dolichos biflorus* agglutinin (DBA)+ pancreatic duct cells but not amylase+ exocrine cells in the ES cell culture (**Supplementary Fig. 6b**). There were no qualitative differences in the expression of the above markers among cells treated with both TBZ and dBu-cAMP or each alone (**Supplementary Fig. 6a,b**). We examined whether the Ins+ cells also expressed other endocrine hormones. Although some Ins-single-positive cells, which do not express other endocrine hormones, exist (approximately 10%) in the culture, over 90% of the Ins+ cells were polyhormonal cells, in which glucagon, somatostatin and/or pancreatic polypeptide were also expressed with insulin (**Supplementary Fig. 6**).

As almost all of the Pdx1+ cells derived from ES cells treated with TBZ or dBu-cAMP expressed insulin at the late stage (day 17), which corresponded to the second phase of Pdx1 expression, where Ins is also coexpressed. (**Fig. 1a**), we purified ES cell–derived *Pdx1*-GFP+ cells by flow cytometry (**Fig. 5a,b**) to analyze the β cells with respect to insulin content, GSIS and mRNA expression (**Fig. 5c–e**). *Pdx1*-GFP+ β cells comprised 10.2% of the total cells recovered (**Fig. 5b**). TBZ alone increased C-peptide content to 10 μg per mg, which is approximately 60% of that in adult islets (**Fig. 5c**). However, TBZ did not promote differentiation into cells capable of GSIS (**Fig. 5d**). Isolated *Pdx1*-GFP+ cells treated with dBu-cAMP alone increased GSIS to 170 ng per mg protein per h, which is 42% of that in mature islets (**Fig. 5d**). However, in contrast to TBZ, dBu-cAMP did not increase C-peptide content on a per-protein level (**Fig. 5d**).

The recovery of C-peptide contents from total ES cell–derived cells treated with TBZ, dBu-cAMP or both compounds is summarized in **Supplementary Figure 7a**. ES cell–derived β cells with a C-peptide content equivalent of approximately 100 islets could be obtained from one 96-well plate. The C-peptide contents increased by approximately 5.7-fold or 2.7-fold through treatment with TBZ or dBu-cAMP alone, respectively, and to 8.1-fold through treatment with both compounds (on a per μg DNA basis). This result is consistent with the above result that TBZ and dBu-cAMP additively increased Ins+ cell number.

We also examined the time-dependent effects of the chemicals on GSIS. TBZ alone did not alter GSIS, but dBu-cAMP alone potentiated ES differentiation into Ins+ cells, showing the ability for GSIS from day 15 (**Supplementary Fig. 7b**). To further confirm that the effect of dBu-cAMP occurs through potentiation of differentiation into Ins+ cells, we treated ES cells with dBu-cAMP in different time windows, that is, from day 11 to day 15 or from day 11 to day 17, and then assayed for GSIS on day 17. Treatment with dBu-cAMP for a longer period (day 11 to day 17) significantly ($P < 0.01$) enhanced GSIS compared to those treated from day 11 to day 15 (**Supplementary Fig. 8**). Treatment with dBu-cAMP during the secretion assay significantly ($P < 0.01$) increased GSIS. Therefore, dBu-cAMP treatment potentiated differentiation into matured β cells and enhanced GSIS ability. The results

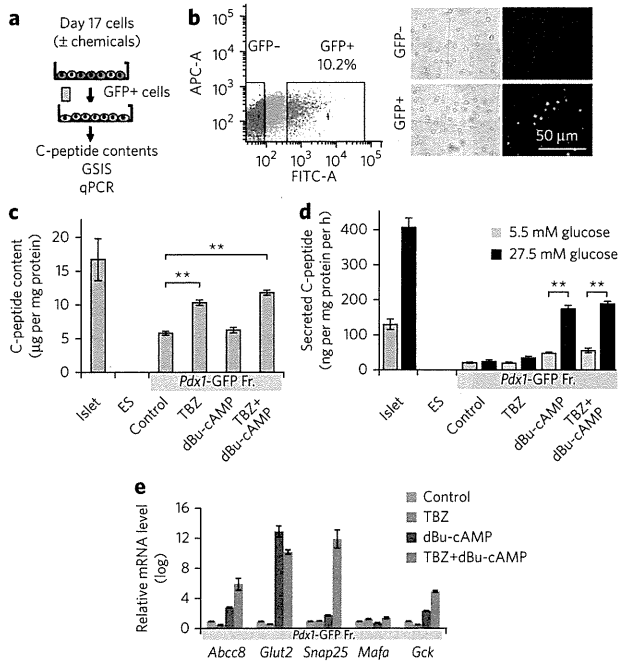

Figure 5 | Characterization of the purified ES cell-derived Ins+ and Pdx-GFP+ cells. TBZ and dBu-cAMP additively potentiated differentiation and maturation of ES cells into β cells with GSIS ability. (**a**–**e**) Differentiated β cells were purified by flow cytometry. Experimental procedures (**a**) and flow cytometry results (**b**) are shown. Cells were tested for their C-peptide contents (**c**), GSIS (**d**) and quantitative PCR (qPCR) (**e**). In **b**, *Pdx1*-GFP+ cells (10.2% of total cells) were purified by flow cytometry on the basis of GFP intensity. Scale bar, 50 μm. In **c** and **d**, treatment with TBZ alone increased C-peptide content, and treatment with dBu-cAMP alone evoked GSIS, as measured by C-peptide contents or secreted C-peptide with significant differences (two-tailed paired Student's *t*-test) $^{**}P < 0.01$. (**e**) Quantitative PCR was performed to quantify the expression of *Abcc8*, *Glut2*, *Snap25*, *Mafa* and *Gck*. In **c**–**e**, GFP+ cells from differentiated ES cells were used, to which DMSO (no chemical treatment), TBZ or dBu-cAMP or both (TBZ + dBu-cAMP) were added. In **c**, $n = 4$, and in **d** and **e**, $n = 3$.

showing that dBu-cAMP potentiated GSIS suggested that the enhancement of differentiation may be mediated by insulin. The effect of insulin was then examined by manipulating the insulin concentration in medium III (**Fig. 1a**), which contained 10 μM insulin in all of the experiments reported so far. Insulin potentiated the differentiation at 16 nM, and its effect declined with increasing insulin concentrations (**Supplementary Fig. 9**). Therefore, TBZ plus dBu-cAMP enhanced insulin secretion at low levels, which in turn accelerated the expression of *Ins1* and further drove β-cell differentiation.

Real-time PCR analyses revealed that dBu-cAMP administration alone increased the expression of genes implicated in GSIS: *Abcc8*, which encodes the regulatory sulfonylurea receptor SUR of the ATP-sensitive potassium channel, and the glucose transporter–encoding genes *Slc2a2* (also known as *Glut2*) and *Gck* (**Fig. 5e**). Double treatment with TBZ and dBu-cAMP upregulated expression of *Abcc8* and *Gck* by ~1×10^5–fold and upregulated expression of *Glut2* and *Snap25*, which encodes a component involved in the regulation of vesicular release, by ~1×10^{10}–fold compared to expression in the control (**Fig. 5e**).

Taken together, these results indicated that TBZ treatment increased insulin content and dBu-cAMP increased GSIS of the ES cell–derived cells. Simultaneous treatment with TBZ and dBu-cAMP enabled the ES cell–derived β cells to produce Ins and secrete Ins *in vitro* in a glucose-sensitive manner at levels comparable to that of adult islets.

The transplanted cells reversed hyperglycemia in mice

To examine their *in vivo* function, we transplanted ES cell–derived β cells into AKITA mice with immunodeficiency (*Rag1*$^{-/-}$ *Ins2*$^{Akita/+}$)[27]. The AKITA mouse is a model that inherits diabetes in a dominant manner owing to a missense mutation in *Ins2*. Consistent with our previous report[28], all male heterogeneous AKITA mice gradually developed hyperglycemia after they reached 6 weeks of age (**Supplementary Fig. 10a**). We harvested 4×10^6 or 1×10^7 ES cell–derived cells (treated with both TBZ and dBu-cAMP) on day 17 and grafted the cells under the kidney capsule in each experimental mouse. The experimental mice showed a reversal of hyperglycemia for more than 6 weeks, with larger grafts showing increasing effects (**Supplementary Fig. 10a**), whereas no change in blood glucose was observed in control untransplanted AKITA mice.

We then transplanted 1×10^7 ES cell–derived cells, which were treated with no chemical, TBZ or dBu-cAMP alone or with both TBZ and dBu-cAMP, into the kidney capsule of the AKITA mice. Mice engrafted with cells that were not treated with growth factors served as negative controls. Mice transplanted with cells treated with TBZ plus dBu-cAMP or dBu-cAMP alone partially recovered from hyperglycemia and showed lowered fasting blood glucose as early as 2 weeks after engraftment (**Fig. 6a**). Mice engrafted with cells treated with both TBZ and dBu-cAMP completely recovered from glucose intolerance, whereas those engrafted with cells treated with dBu-cAMP alone did not (**Fig. 6a–c**). In both cases, the engrafted mice showed even higher levels of plasma C-peptide compared to that in the control wild-type BL6 mice (**Supplementary Fig. 10b**). The AKITA mice are reported to be insulin resistant[29]. The above results might reflect the insulin resistance of the recipient AKITA mice. In contrast, mice engrafted with cells treated with TBZ alone responded to glucose administration and increased plasma C-peptide levels more rapidly compared to those engrafted with control cells (no chemical treatment) (**Supplementary Fig. 10b**), which agreed with their partial reversal of glucose tolerance (**Fig. 6b**) and fasting blood glucose (**Fig. 6a**).

Grafts without noticeable tumor formation were recovered from the experimental mice and were found to express insulin (**Supplementary Fig. 10c**). No insulin-positive cells coexpressed glucagon, pancreas polypeptide or somatostatin. We confirmed that the β-cell mass in the recipient AKITA pancreas did not increase after transplantation, showing an altered allocation of glucagon+ cells at the center of the islets, in contrast to their peripheral localization in the control wild-type mice (**Supplementary Fig. 10d**). Taken together, we concluded that the reversal of hyperglycemia and restoration of glucose tolerance was due to the transplanted ES cell–derived cells.

These results demonstrate that treatment of both TBZ and dBu-cAMP potentiated differentiation of ES cells into cells, with a high level of C-peptide contents and GSIS ability, and transplantation of these cells reversed hyperglycemia in AKITA diabetic mice.

DISCUSSION

Although the function of VMAT2 in the pancreas is largely unknown, VMAT2 is known to take up monoamines such as dopamine, histamine and serotonin into secretory granules of neurons and exert both autocrine and paracrine functions in the nervous system. VMAT2 is described to be expressed in human β cells. However, there has been some controversy in the literature about its presence in β cells of rodents[30]. Here, the target cells of the VMAT2 inhibitors are differentiating pancreatic progenitor cells. We revealed a new role of VMAT2 and monoamine-dependent suppression of differentiation from the pancreatic progenitor cells.

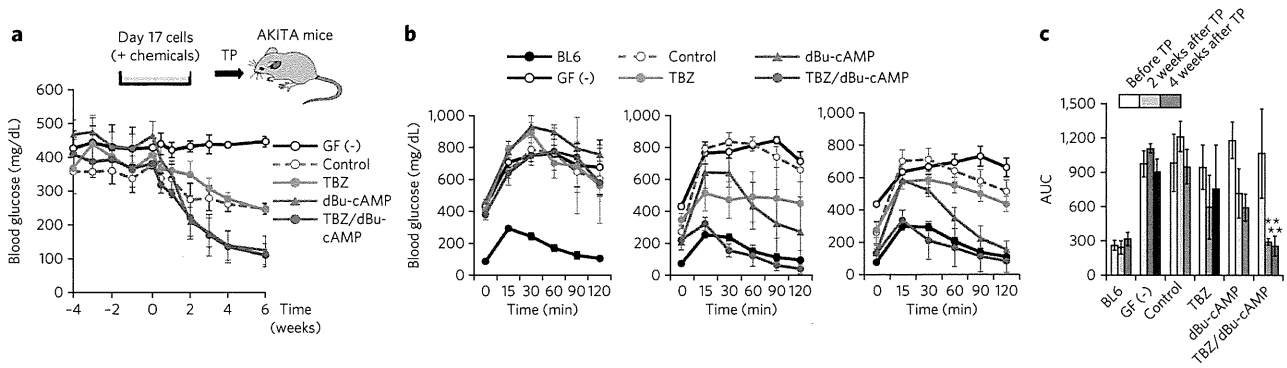

Figure 6 | Transplanted cells reversed hyperglycemia and glucose tolerance. Transplantation assays showed that the induced β cells normalized fasting blood glucose levels and glucose tolerance in the AKITA diabetic mice. (**a**) Top, experimental procedure. *In vitro* differentiated β cells, treated with TBZ and dBu-cAMP, were harvested on day 17 and transplanted into hyperglycemic AKITA mice. Bottom, fasting blood glucose levels (mg/dL) of mice transplanted with ES-derived β cells were measured before and after engraftment. X axis shows weeks after transplantation. (**b**) AKITA mice were analyzed for IPGTT before engraftment (left), 2 weeks (middle) or 4 weeks (right) after engraftment, and time courses of blood glucose levels (mg/dL) after challenge with glucose are shown. X axis shows minutes after glucose challenges. (**c**) Area under curve (AUC) of IPGTT curves shown in **b**. Light color bars, before engraftment; darker color bars, 2 weeks after engraftment; darkest color bars, 4 weeks after engraftment. In **a** and **b**, blue circles represent treatment with TBZ, green circles represent treatment with dBu-cAMP, purple circles represent treatment with TBZ and dBu-cAMP, broken lines with open circles represent no chemical treatment at 1×10^7, and black lines with open circles represent cells with no growth factor treatment (negative controls). In **a**–**c**, the significant differences between treatment and control were $^*P < 0.05$ or $^{**}P < 0.01$ (two-tailed unpaired Student's *t*-test) and are indicated above error bars, which show s.d.

Dopamine, histamine and serotonin are synthesized and stored in the endocrine pancreas during pregnancy[31] and in adult β cells[19]. In the adult, there are several lines of evidence supporting that dopamine and histamine negatively regulate insulin content, glucose tolerance[32–34] and GSIS[35–37]. In contrast, serotonin is reported to drive β-cell replication and regulate glucose tolerance in pregnant mice. However, the role of monoamines during embryonic development remains largely unknown.

Among the monoamines, dopamine is produced at a highest level in ES cell–derived cells and during embryonic stages. Consistent with this, dopamine synthesizing enzyme (encoded by *Th*), was expressed in the ES-derived cells at a level comparable to that in the embryonic pancreas. In spite of the differences in their cellular contents, inhibition of all three synthesizing enzymes showed similar effects to enhance β-cell differentiation, indicating that all of these monoamines take part in this process. It was puzzling that application of these monoamines dose-dependently suppressed β cell differentiation with similar EC_{50} values, although their EC_{50} against their specific receptors are very different[38–40]. We hypothesize that this is due to the fact that monoamine is taken up into the storage vesicles and their subsequent release is required for their action and that other components co-released from the vesicle might be required to convey their function[41].

Our results indicated that monoamines controlled by VMAT2 serve as a brake for differentiation of Pdx1+ pancreatic progenitors into Ngn3+ endocrine precursors and subsequently into Ins+ cells. Once this brake is released, the Pdx1+ cells are induced to differentiate into Ngn3+ cells, which quickly turn into Ins+ cells. TBZ acted during a short time window to increase Ngn3+ cells, suggesting that this brake functions transiently. However, whether there are specific roles for each of the monoamines remains an open question.

In the adult β cells, GLP1 and GIP are well known to activate $G\alpha_s$-coupled receptors and potentiate GSIS by activating cAMP signaling and modulating K_{ATP} channel activity. It is reported that cAMP signaling induces glucose responsiveness through both PKA and Epac2 dependent pathway[23]. PKA is reported to modulate VMAT2 by regulating its trafficking[42]. It is possible that cAMP activates β-cell differentiation through modulating VMAT2. It remains unknown whether GLP1, GIP or other unknown ligands function to promote the maturation of β cells to initiate GSIS during embryonic development. This would agree with the observation that pancreas-specific $G\alpha_s$-deficient mice demonstrated reduced β-cell mass and defects in glucose response[43].

Most of the ES cell–derived insulin+ cells were polyhormonal cells, coexpressing other endocrine hormones. Maturation rapidly occurred *in vivo*. They rapidly turned into insulin-single positive cells after they were grafted under kidney capsules. Intrapenitoneal glucose trelant test (IPGTT) results revealed that cells doubly treated with TBZ and dBu-cAMP matured into cells capable of GSIS and restored glucose tolerance as early as 2 weeks after engraftment. Cells treated with TBZ alone or with no chemicals also matured *in vivo* and became potent for GSIS within 2 weeks. In mouse pancreatic development, Ins+ glucagon+ cells appear early in 'first transition', and they do not contribute to the generation of mature β cells[44]. These cells do not express mature endocrine markers[45]. By contrast, Ins+ glucagon+ transitional cells exist transiently during the conversion of α cells into β cells[46,47]. The polyhormonal cells observed in the present study expressed mature endocrine markers. Therefore, the ES cell–derived polyhormonal cells here might have characteristics close to the transitional cells that appear during cell fate conversion rather than those that exist during early mouse embryonic development. Although the exact mechanism of how ES cells mature under *in vivo* environment remains unknown, it is reported that dynamic chromatin remodeling occurs in human ES cells after they are engrafted *in vivo*[48]. Previous studies have shown that human ES cell–derived insulin-expressing cells, which are polyhormonal, differentiate into α cells, instead of β cells, after transplantation[49]. The discrepancies might be due to the differences in the underlying mechanism between the mouse and human ES cells or due to the differences between the culture protocols. However, it is technically difficult for us to perform further long-term analyses, such as transplantation or re-culture of the mouse ES cell–derived Pdx1/GFP+ cells, owing to a significant ($P < 0.01$) loss of cell viability after sorting at this late stage of differentiation. Taken together, although we cannot completely rule out other possibilities, our results suggested that the transplanted insulin-expressing cells reversed hyperglycemia in AKITA mice.

The graft experiments showed that transplanting 4×10^6 or 1×10^7 ES cell–derived cells, with their C-peptide contents equivalent to 40 or 100 islets, respectively, is enough to reverse hyperglycemia in AKITA diabetic mice. This is lower than the previously reported observation that it is necessary to transplant 150–200 islets to reverse hyperglycemia[50]. Our results suggested that these ES cell–derived cells rapidly underwent further differentiation *in vivo* and increased their C-peptide contents or GSIS ability so that a lower number of ES cell–derived cells was enough for the reversal of hyperglycemia.

The ES cell–derived cells showed no signs of tumor formation. This might due to the high differentiation efficiency into the definitive endoderm. Moreover, the long differentiation period might also result in a low population of undifferentiated cells remaining in culture.

In conclusion, results of the present study demonstrated a previously unknown function of VMAT2 in controlling differentiation into pancreatic endocrine precursors. VMAT2 inhibition and dBu-cAMP addition synergized and further increased *Ins1* transcripts and are sufficient to promote differentiation of ES cells into functional β cells capable of reversing hyperglycemia in diabetic mice. Future studies would be required to analyze the role of VMAT2 during human induced pluripotent stem cell cell differentiation to apply this protocol for future cell replacement therapy.

Received 15 December 2012; accepted 15 October 2013; published online 15 December 2013

METHODS

Methods and any associated references are available in the online version of the paper.

References

1. Jonsson, J., Carlsson, L., Edlund, T. & Edlund, H. Insulin-promoter-factor 1 is required for pancreas development in mice. *Nature* **371**, 606–609 (1994).
2. Gu, G., Dubauskaite, J. & Melton, D.A. Direct evidence for the pancreatic lineage: NGN3+ cells are islet progenitors and are distinct from duct progenitors. *Development* **129**, 2447–2457 (2002).
3. Gradwohl, G., Dierich, A., LeMeur, M. & Guillemot, F. *neurogenin3* is required for the development of the four endocrine cell lineages of the pancreas. *Proc. Natl. Acad. Sci. USA* **97**, 1607–1611 (2000).
4. Puri, S. & Hebrok, M. Cellular plasticity within the pancreas—lessons learned from development. *Dev. Cell* **18**, 342–356 (2010).
5. D'Amour, K.A. *et al.* Efficient differentiation of human embryonic stem cells to definitive endoderm. *Nat. Biotechnol.* **23**, 1534–1541 (2005).
6. Skoudy, A. *et al.* Transforming growth factor (TGF)β, fibroblast growth factor (FGF) and retinoid signalling pathways promote pancreatic exocrine gene expression in mouse embryonic stem cells. *Biochem. J.* **379**, 749–756 (2004).
7. D'Amour, K.A. *et al.* Production of pancreatic hormone-expressing endocrine cells from human embryonic stem cells. *Nat. Biotechnol.* **24**, 1392–1401 (2006).
8. Borowiak, M. *et al.* Small molecules efficiently direct endodermal differentiation of mouse and human embryonic stem cells. *Cell Stem Cell* **4**, 348–358 (2009).
9. Chen, S. *et al.* A small molecule that directs differentiation of human ESCs into the pancreatic lineage. *Nat. Chem. Biol.* **5**, 258–265 (2009).
10. Shiraki, N. *et al.* Guided differentiation of embryonic stem cells into Pdx1-expressing regional-specific definitive endoderm. *Stem Cells* **26**, 874–885 (2008).
11. Higuchi, Y. *et al.* Synthesized basement membranes direct the differentiation of mouse embryonic stem cells into pancreatic lineages. *J. Cell Sci.* **123**, 2733–2742 (2010).
12. Wang, Y.M. *et al.* Knockout of the vesicular monoamine transporter 2 gene results in neonatal death and supersensitivity to cocaine and amphetamine. *Neuron* **19**, 1285–1296 (1997).
13. Pothos, E.N. *et al.* Synaptic vesicle transporter expression regulates vesicle phenotype and quantal size. *J. Neurosci.* **20**, 7297–7306 (2000).
14. Vergo, S., Johansen, J.L., Leist, M. & Lotharius, J. Vesicular monoamine transporter 2 regulates the sensitivity of rat dopaminergic neurons to disturbed cytosolic dopamine levels. *Brain Res.* **1185**, 18–32 (2007).
15. Eiden, L.E. & Weihe, E. VMAT2: a dynamic regulator of brain monoaminergic neuronal function interacting with drugs of abuse. *Ann. NY Acad. Sci.* **1216**, 86–98 (2011).
16. Erickson, J.D., Schafer, M.K., Bonner, T.I., Eiden, L.E. & Weihe, E. Distinct pharmacological properties and distribution in neurons and endocrine cells of two isoforms of the human vesicular monoamine transporter. *Proc. Natl. Acad. Sci. USA* **93**, 5166–5171 (1996).
17. Anlauf, M. *et al.* Expression of the two isoforms of the vesicular monoamine transporter (VMAT1 and VMAT2) in the endocrine pancreas and pancreatic endocrine tumors. *J. Histochem. Cytochem.* **51**, 1027–1040 (2003).
18. Simpson, N.R. *et al.* Visualizing pancreatic β-cell mass with [^{11}C]DTBZ. *Nucl. Med. Biol.* **33**, 855–864 (2006).
19. Saisho, Y. *et al.* Relationship between pancreatic vesicular monoamine transporter 2 (VMAT2) and insulin expression in human pancreas. *J. Mol. Histol.* **39**, 543–551 (2008).
20. Grimsby, J., Chen, K., Wang, L.J., Lan, N.C. & Shih, J.C. Human monoamine oxidase A and B genes exhibit identical exon-intron organization. *Proc. Natl. Acad. Sci. USA* **88**, 3637–3641 (1991).
21. Gu, G. *et al.* Global expression analysis of gene regulatory pathways during endocrine pancreatic development. *Development* **131**, 165–179 (2004).
22. Kroeze, W.K., Sheffler, D.J. & Roth, B.L. G-protein-coupled receptors at a glance. *J. Cell Sci.* **116**, 4867–4869 (2003).
23. Seino, S., Shibasaki, T. & Minami, K. Dynamics of insulin secretion and the clinical implications for obesity and diabetes. *J. Clin. Invest.* **121**, 2118–2125 (2011).
24. Lo, K.W., Kan, H.M., Ashe, K.M. & Laurencin, C.T. The small molecule PKA-specific cyclic AMP analogue as an inducer of osteoblast-like cells differentiation and mineralization. *J. Tissue Eng. Regen. Med.* **6**, 40–48 (2012).
25. Mei, F.C. *et al.* Differential signaling of cyclic AMP: opposing effects of exchange protein directly activated by cyclic AMP and cAMP-dependent protein kinase on protein kinase B activation. *J. Biol. Chem.* **277**, 11497–11504 (2002).
26. Kelley, G.G. *et al.* Glucose-dependent potentiation of mouse islet insulin secretion by Epac activator 8-pCPT-2′-*O*-Me-cAMP-AM. *Islets* **1**, 260–265 (2009).
27. Wang, J. *et al.* A mutation in the insulin 2 gene induces diabetes with severe pancreatic β-cell dysfunction in the *Mody* mouse. *J. Clin. Invest.* **103**, 27–37 (1999).
28. Mochida, T. *et al.* Time-dependent changes in the plasma amino acid concentration in diabetes mellitus. *Mol. Genet. Metab.* **103**, 406–409 (2011).
29. Hong, E.G. *et al.* Nonobese, insulin-deficient Ins2Akita mice develop type 2 diabetes phenotypes including insulin resistance and cardiac remodeling. *Am. J. Physiol. Endocrinol. Metab.* **293**, E1687–E1696 (2007).
30. Schäfer, M.K. *et al.* Species-specific vesicular monoamine transporter 2 (VMAT2) expression in mammalian pancreatic β cells: implications for optimising radioligand-based human β cell mass (BCM) imaging in animal models. *Diabetologia* **56**, 1047–1056 (2013).
31. Harris, P.E. *et al.* VMAT2 gene expression and function as it applies to imaging β-cell mass. *J. Mol. Med.* **86**, 5–16 (2008).
32. Fülöp, A.K. *et al.* Hyperleptinemia, visceral adiposity, and decreased glucose tolerance in mice with a targeted disruption of the histidine decarboxylase gene. *Endocrinology* **144**, 4306–4314 (2003).
33. Buchanan, T.A. & Xiang, A.H. Gestational diabetes mellitus. *J. Clin. Invest.* **115**, 485–491 (2005).
34. Kim, H. *et al.* Serotonin regulates pancreatic β cell mass during pregnancy. *Nat. Med.* **16**, 804–808 (2010).
35. Rubí, B. *et al.* Dopamine D2-like receptors are expressed in pancreatic β cells and mediate inhibition of insulin secretion. *J. Biol. Chem.* **280**, 36824–36832 (2005).
36. Ericson, L.E., Hakanson, R. & Lundquist, I. Accumulation of dopamine in mouse pancreatic B-cells following injection of l-DOPA. Localization to secretory granules and inhibition of insulin secretion. *Diabetologia* **13**, 117–124 (1977).
37. Zern, R.T., Bird, J.L. & Feldman, J.M. Effect of increased pancreatic islet norepinephrine, dopamine and serotonin concentration on insulin secretion in the golden hamster. *Diabetologia* **18**, 341–346 (1980).
38. Seeman, P. *et al.* The dopaminergic stabilizer ASP2314/ACR16 selectively interacts with $D2^{High}$ receptors. *Synapse* **63**, 930–934 (2009).
39. Braden, M.R., Parrish, J.C., Naylor, J.C. & Nichols, D.E. Molecular interaction of serotonin 5-HT2A receptor residues $Phe339^{(6.51)}$ and $Phe340^{(6.52)}$ with superpotent *N*-benzyl phenethylamine agonists. *Mol. Pharmacol.* **70**, 1956–1964 (2006).
40. Peakman, M.C. & Hill, S.J. Endogenous expression of histamine H1 receptors functionally coupled to phosphoinositide hydrolysis in C6 glioma cells: regulation by cyclic AMP. *Br. J. Pharmacol.* **113**, 1554–1560 (1994).
41. El Mestikawy, S., Wallen-Mackenzie, A., Fortin, G.M., Descarries, L. & Trudeau, L.E. From glutamate co-release to vesicular synergy: vesicular glutamate transporters. *Nat. Rev. Neurosci.* **12**, 204–216 (2011).
42. Yao, J., Erickson, J.D. & Hersh, L.B. Protein kinase A affects trafficking of the vesicular monoamine transporters in PC12 cells. *Traffic* **5**, 1006–1016 (2004).
43. Xie, T., Chen, M. & Weinstein, L.S. Pancreas-specific Gs_α deficiency has divergent effects on pancreatic α- and β-cell proliferation. *J. Endocrinol.* **206**, 261–269 (2010).

44. Herrera, P.L. Adult insulin- and glucagon-producing cells differentiate from two independent cell lineages. *Development* **127**, 2317–2322 (2000).
45. Murtaugh, L.C. Pancreas and β-cell development: from the actual to the possible. *Development* **134**, 427–438 (2007).
46. Collombat, P. *et al.* The ectopic expression of Pax4 in the mouse pancreas converts progenitor cells into alpha and subsequently β cells. *Cell* **138**, 449–462 (2009).
47. Thorel, F. *et al.* Conversion of adult pancreatic α-cells to β-cells after extreme β-cell loss. *Nature* **464**, 1149–1154 (2010).
48. Xie, R. *et al.* Dynamic chromatin remodeling mediated by polycomb proteins orchestrates pancreatic differentiation of human embryonic stem cells. *Cell Stem Cell* **12**, 224–237 (2013).
49. Kelly, O.G. *et al.* Cell-surface markers for the isolation of pancreatic cell types derived from human embryonic stem cells. *Nat. Biotechnol.* **29**, 750–756 (2011).
50. Yasunami, Y. *et al.* Vα14 NK T cell-triggered IFN-γ production by Gr-1+CD11b+ cells mediates early graft loss of syngeneic transplanted islets. *J. Exp. Med.* **202**, 913–918 (2005).

Acknowledgments

We thank members of the Gene Technology Center and Center for Animal Resources and Development at Kumamoto University for technical assistance. This work was supported by the Funding Program for Next Generation World-Leading Researchers (to S.K. (no. LS099) and M.U.); the Japan Society for the Promotion of Science, the Realization of Regenerative Medicine (to S.K. and M.U.); the Program for Leading Graduate Schools 'HIGO' (awarded to S.K.); Grants-in-Aid from the Ministry of Education, Culture, Sports, Science and Technology (MEXT), Japan (no. 21390280 to S.K. and no. 22790653 to D. Sakano); and the Collaborative Research Program of Institute for Chemical Research, Kyoto University (grant no. 2010-44). The iCeMS is supported by World Premier International Research Center Initiative, MEXT, Japan.

Author contributions

D. Sakano performed chemical screening, cellular and biochemical analyses; D. Sakano, N.S. and K.U. established the ES cell differentiation system; D. Sakano, K. Kikawa, M.K. and T.Y. performed transplantation assays; K.A. established the ES cell line; S.M., F.E. and N.N. helped maintain AKITA mice; D.M. and M.U. provided and analyzed the chemical library; O.A. and D. Stainier provided chemicals; K. Kume and S.K. provided technical advices, S.K. designed the experiments and wrote the paper. All of the authors discussed the results and commented on the manuscript.

Competing financial interests

The authors declare no competing financial interests.

Additional information

Supplementary information and chemical compound information is available in the online version of the paper. Reprints and permissions information is available online at http://www.nature.com/reprints/index.html. Correspondence and requests for materials should be addressed to S. Kume.

ONLINE METHODS

Ethics statement. This animal work is approved by the Institutional Review Board for Animal Care and Use of Kumamoto University. All animal procedures were conducted according to Kumamoto University guideline.

ES cell lines. The SK7 ES cell line[10] was established from a transgenic mouse line bearing the *Pdx1*-GFP gene. NGP9 ES cells were established by culturing blastocysts obtained from transgenic mice heterozygous for the *Ngn3*-GFP gene[21]. SK7 and NGP9 cells were maintained on MEF feeder cells in Dulbecco's modified Eagle's medium (DMEM; Invitrogen, Carlsbad, CA) supplemented with leukemia inhibitory factor (LIF), 10% FBS, nonessential amino acids (NEAA), L-glutamine (L-Gln), penicillin and streptomycin (PS) and β-mercaptoethanol (β-ME)[10].

Differentiation of ES cells into pancreatic β cells. For differentiation studies, ES cells were plated at 5,000 cells per well, in Corning 96-well plates with Ultra-Web Synthetic Polyamine Surface (no. 3873XX1, Corning Coster, Cambridge, MS). The cells were cultured for 7 d in Medium I: Dulbecco's Modified Eagle Medium (DMEM: Invitrogen, Glasgow, UK) containing 4,500 mg/L glucose and supplemented with 100 μM nonessential amino acids (NEAA), 2 mM L-glutamine (L-Gln; Nacalai tesque, Japan), 1 mM sodium pyruvate (Invitrogen), 50 units/mL penicillin, 50 μg/mL streptomycin (PS; Nacalai tesque), 100 μM β-mercaptoethanol (β-ME; Sigma-Aldrich), ITS (10 μg/mL insulin (Sigma-Aldrich), 5.5 μg/mL transferrin (Sigma-Aldrich) and 6.7 pg/mL selenium (Sigma-Aldrich)), 0.25% Albmax (Invitrogen), 10 ng/ml recombinant human Activin-A (R&D Systems, Minneapolis, MN) and 5 ng/mL recombinant human bFGF (Peprotech). On days 7–11, the cells were cultured in Medium II: RPMI 1640 medium (Invitrogen) containing 2,000 mg/L glucose (Sigma, St. Louis, MO), 1 μM retinoic acid (Sigma-Aldrich), 50 ng/mL human recombinant fibroblast growth factor-10 (human recombinant FGF10, Peprotech, Rocky Hill, NJ), 2% B-27 Supplement (Invitrogen) and 0.25 μM of the Shh signaling antagonist 3-keto-*N*-(aminoethyl-aminocaproyl-dihydrocinnamoyl) cyclopamine (KAAD-cyclopamin, Calbiochem, San Diego, CA). Finally, on days 11–17, cells were cultured in Medium III: DMEM containing 1,000 mg/L glucose supplemented with NEAA, L-Gln, PS, β-ME, ITS, 0.25% Albmax (Invitrogen), 10 nM glucagon-like peptide 1 (GLP-1, Sigma-Aldrich) and 10 mM nicotinamide (NA, Sigma-Aldrich). The medium was replaced every 2 d.

Screening of small molecules and quantitative analysis of imaging. Small molecules from the bioactive, pharmacologically defined Prestwick Chemical Library were screened for pro-differentiation factors. Compounds were dissolved in DMSO (Sigma-Aldrich) and added at 1:100 on day 11, with changes on days 13 and 15. Cells were assayed by immunostaining with mouse anti-insulin (Sigma-Aldrich; I2018; 1:1,000) on day 17. Fluorescent images were quantified by counting pixel numbers representing the number of positive cells, using a ImageXpress Micro scanning system and MetaXpress cellular image analysis software (Molecular Devices, Japan). Data were normalized as fold change relative to DMSO controls. Hit compounds were defined as causing a twofold or higher increase in insulin-positive β cells. Candidate compounds were tested for dose dependency and reproducibility. The screening information is summarized in **Supplementary Table 1**.

Chemicals. Reserpine was purchased from Calbiochem Novabiochem Novagen, TBZ was purchased from Tocris Bioscience, and dibutyryl-cAMP (dBu-cAMP) was purchased from BIOMOL International.

Pargyline was purchased from Cayman Chemicals. The compounds were dissolved in DMSO (final concentration = 1.0%) and added on days 11, 13 and 15. After initial screening, the following concentrations were used: 0.63 μM reserpine, 1.25 μM TBZ, 0.1 μM dopamine (LKT Labs, Inc.), 0.6 μM dBu-cAMP, 1.0 μM pargyline, 1.3 μM α-methyltyrosine (α-MT, Sigma-Aldrich), 0.6 μM L-3,4-dihydroxyphenylalanine (L-DOPA, Toronto Research Chemicals Inc,), 1.3 μM α-fluoromethyl- histidine (α-FMH, Toronto Research Chemicals Inc,), 1.3 μM 5-hydroxy tryptophan (5HTP, Sigma-Aldrich) and 0.6 μM carbachol (Sigma-Aldrich), unless otherwise specified.

Chemical characterization. To confirm the purity of reserpine, TBZ and dBu-cAMP, we checked their HPLC, LC-MS (ESI), and ^{1}H-NMR profiles. The results showed that the reagents we used had high purity (>90%) (**Supplementary Figs. 11–13**). HPLC analysis was performed with a Shimadzu LC-2010C equipped with reversed-phase HPLC column (GL science, Inertsil ODS-3, 4.6 × 150 mm, flow rate 1.0 mL/min, 0.1% TFA CH_3CN/H2O, 10–100%). Mass spectra (ESI) were recorded on a Shimadzu LCMS-2010. ^{1}H-NMR spectra were collected on a JEOL JNM-ECP (300 MHz).

Immunocytochemistry. For immunocytochemistry, ES cells were fixed with 4% paraformaldehyde and processed after 13 days in culture (**Fig. 3** and **Supplementary Fig. 5**), 17 d in culture (**Figs. 1, 2** and **4** and **Supplementary Fig. 6**) or 6 weeks after transplantation (**Supplementary Fig. 10**). For examination of target protein expression in single cells, ES cell–derived differentiated cells were dissociated with 0.25% trypsin (Invitrogen), replated for 30 min and then fixed and processed for immunocytochemistry. The following antibodies were used: rabbit anti-MafA (Abcam; ab17976; 1/100,), rabbit anti–C-peptide (Cell Signaling; 4593, 1/100), guinea pig anti-insulin (Dako; A0564; 1/1,000), rabbit anti-pancreatic polypeptide (Dako; A619; 1/100), mouse anti-Nkx2.2 (Developmental Studies Hybridoma Bank, University of Iowa; 74.5A5; 1/100), mouse anti-Nkx6.1 (Developmental Studies Hybridoma Bank, University of Iowa; F64A6B4; 1/100), rabbit anti-GFP (MBL International Corp; 598; 1/1,000), goat anti-Pdx1 (R&D systems; AF2419, 1/100), goat anti-amylase (Santa Cruz Biotechnology; sc-12821; 1/100), goat anti-somatostatin (Santa Cruz Biotechnology; sc-7819; 1/100), mouse anti-glucagon (Sigma-Aldrich; G2654; 1/1,000), biotin-conjugated *D. biflorus* agglutinin (DBA) lectin (Sigma-Aldrich; L6533; 1/500) and mouse anti-insulin (Sigma-Aldrich; I2018; 1/1,000) antibodies were used. Secondary antibodies used were Alexa 488–conjugated goat anti-mouse IgG (A11029; 1/1,000), Alexa 568–conjugated goat anti-guinea pig IgG (A11075; 1/1,000), Alexa 568–conjugated goat anti-mouse IgG (A11031; 1/1,000), Alexa 568–conjugated goat anti-rabbit IgG (A11036; 1/1,000), Alexa 568–conjugated anti-streptabidine antibody (S11223; 1/1,000), or Alexa 633–conjugated donkey anti-goat IgG (A21082; 1/1,000), Alexa 633–conjugated goat anti-mouse IgG (A21053; 1/1,000), Alexa 633–conjugated goat anti-rabbit IgG (A21072; 1/1,000) (all from Invitrogen). Cells were counterstained with DAPI (Roche Diagnotics, Basel, Switzerland).

Gene silencing. In the VMAT2-knockdown assays, cells were transfected with Expression Arrest nonsilencing, control shRNA (Open Biosystems, no. RHS4080), VMAT2 shRNA (Open Biosystems, no. RMM3981-97058457 and no. RMM3981-97058458). The lentiviral vectors were constructed as previously described[11]. SK7 cells were infected with viral supernatants. After 24 h of incubation, the virus-containing medium was replaced with fresh ES maintenance medium. After 24 h of incubation, infected cells were selected using 1.5 μg/mL puromycin (Sigma-Aldrich). The surviving cells were harvested, and clones were selected to establish knockdown and control cell lines.

Measurement of intracellular monoamine levels. Cells were treated with chemicals before harvest (days 11–17). Cells were lysed with lysis buffer containing 0.1% Triton X-100 (Nakarai Tesque, Japan) in 0.1 M PBS (pH7.2, Sigma-Aldrich) with protease inhibitor cocktail. Lysates were assayed for dopamine, histamine, serotonin, adrenaline or noradrenaline with each monoamine-specific ELISA kit (Labor Diagnostika Nord GmbH & Co.; KG Nordhorn Germany).

EdU incorporation. Cells were treated with culture medium containing 20 μM 5-ethynyl-2′-deoxyuridine (EdU) for 48 h before harvest (days 17–19), processed using the Click-iT EdU Alexa Fluor 594 Imaging Kit (Invitrogen) and stained with DAPI and anti-GFP antibodies, rabbit anti-GFP (no. 598; 1:1,000; MBL International Corp., Woburn, MA) and detected with Alexa 488-conjugated goat anti-rabbit IgG (Invitrogen; A-11008; 1:1,000).

Pancreas bud *in vitro* culture. Pancreas buds were dissected from E12.5 embryos of a transgenic mouse line bearing the *Pdx1*- green fluorescent protein (GFP) gene. The tissue was placed onto 12-well Corning Transwell cell culture inserts (Corning Coster, Cambridge, MS). The bottom of the inserts were touched with medium containing M199 with NEAA, L-Gln, PS, β-ME and 10% FBS (FBS, Hyclone).

Flow cytometry. Cells were collected and suspended in 1 × HANKS with 1% FBS. A FACS Aria II flow cytometry cell sorter (Becton Dickinson Immunocytometry Systems, San Jose, CA) was used to purify GFP-positive cells by sorting them against the fluorescence profiles of differentiating cells prepared from wild-type mice. Dead cells were identified using propidium iodide (Sigma-Aldrich).

Quantitative real-time PCR. RNA was extracted from ES cells, mouse tissue or transplanted grafts using the RNeasy minikit (Qiagen, Hilden, Germany) and then treated with DNase I (Qiagen).

Complementary DNA was synthesized from 1 μg of total RNA using Revertra Ace qPCR RT Master Mix (Toyobo).

For real-time PCR analysis, the mRNA expression was quantified with SyberGreen on an ABI 7500 thermal cycler (Applied Biosystems, Foster City, CA). The level of expression of each gene was normalized with that of the β-actin–expressing gene *Actb* . The PCR conditions were as follows: denaturation at 95 °C for 15 s, annealing and extension at 60 °C for 60 s for up to 40 cycles. Each measurement was normalized to *Actb* (mouse) expression for each sample by subtracting the average *Actb* (mouse) expression. C_t values (threshold cycle) from the average Each gene C_t, resulting in C_t Target mRNA levels are expressed as arbitrary units. All of the primers for real-time PCR are listed in **Supplementary Table 2**.

Measurement of glucose-stimulated C-peptide secretion and cellular or plasma C-peptide level by enzyme-linked immunosorbent assay. Differentiating ES cells were preincubated for 0.5 h in low glucose (5.5 mM) DMEM with minimal essential medium and 1% FBS. Cells were washed twice with phosphate-buffered saline then incubated for 2 h in low-glucose (5.5 mM) or high-glucose (27.5 mM) DMEM with 1% FBS. The culture medium was collected, and cells were lysed with a lysis buffer of 0.1% Triton X-100 in PBS with added protease inhibitor cocktail. Insulin secretion into the culture medium and insulin content of the cell lysates were measured using a mouse C-peptide ELISA kit (Shibayagi Co. Ltd., Japan).

IPGTT. Mice fasted for 16–18 h were used. Body weights were measured. Blood glucose levels were measured before (0 min) or at 15 min, 30 min, 60 min, 90 min and 120 min after intraperitoneal administration of 25% Glucose (Sigma-Aldrich) solution at 2 g per kg body weight. Serum C-peptide concentrations were measured as described above.

Cell transplantation into AKITA mice. Differentiated cells were dissociated with 0.25% trypsin, resuspended in DMEM with 10% FBS and injected under the kidney capsules of AKITA mice (C57BL/6J-*Rag1*$^{-/-}$*Ins2*$^{Akita/+}$; male)[27] with a 24G catheter (NIPRO, Japan). The AKITA mice were at least 6 weeks old. Six weeks after transplantation, the tissue was removed and analyzed for insulin expression, content and secretion, as described above.

Statistical tests. Data were analyzed by two-tailed *t*-test. Data are presented as mean ± s.d.

doi:10.1038/nchembio.1410

Category of manuscript: **Original Article**

Title: **Molecular diagnosis of mitochondrial respiratory chain disorders in Japan: Focusing on mitochondrial DNA depletion syndrome**

Running title: **mitochondrial respiratory chain disorders in Japan**

Taro Yamazaki, MD[a,b], Kei Murayama, MD, PhD[c], Alison G. Compton, PhD[b], Canny Sugiana, PhD[b,#], Hiroko Harashima, BSc[a], Shin Amemiya, MD, PhD[a], Masami Ajima, BSc[c], Tomoko Tsuruoka, MD[c], Ayako Fujinami, MD[c], Emi Kawachi, MD[c], Yoshiko Kurashige, MD[d], Kenshi Matsushita, MD, PhD[d], Hiroshi Wakiguchi, MD, PhD[d], Masato Mori, MD, PhD[e], Hiroyasu Iwasa, MD, PhD[f], Yasushi Okazaki, MD, PhD[f], David R. Thorburn, PhD[b] and Akira Ohtake, MD, PhD[a,*]

[a]Department of Pediatrics, Faculty of Medicine and [f]Translational Research Center, International Medical Center, Saitama Medical University, Saitama, JAPAN

This article has been accepted for publication and undergone full peer review but has not been through the copyediting, typesetting, pagination and proofreading process, which may lead to differences between this version and the Version of Record. Please cite this article as doi: 10.1111/ped.12249

[b]Murdoch Childrens Research Institute, Royal Children's Hospital & Department of Paediatrics, University of Melbourne, Melbourne, AUSTRALIA

[c]Department of Metabolism, Chiba Children's Hospital, Chiba, JAPAN

[d]Department of Pediatrics, Kochi Medical School Kochi University, Kochi, JAPAN

[e]Department of Pediatrics, Jichi Medical University, Tochigi, JAPAN

[#]Present Address:

Canny Sugiana

Monash IVF PTY Ltd, Melbourne, AUSTRALIA

*Corresponding author: Akira Ohtake MD, PhD, Professor, Department of Pediatrics, Faculty of Medicine, Saitama Medical University

38 Morohongo, Moroyama, Iruma-gun, Saitama, 350-0495 JAPAN

TEL:+49-276-1218, FAX:+49-276-1790

E-mail: akira_oh@saitama-med.ac.jp